Environmental Chemistry
2018, Volume 15 Issue 1-2 Pages 58-73
http://dx.doi.org/10.1071/EN17150
http://archimer.ifremer.fr/doc/00444/55558/

On the nature of dissolved copper ligands in the early buoyant plume of hydrothermal vents

Cotte Laura [1, 2, *], Omanovic Dario [3], Waeles Mathieu [2], Laes Agathe [4], Cathalot Cecile [5], Sarradin Pierre-Marie [1], Riso Ricardo D. [2]

[1] IFREMER, Lab Environm Profond LEP EEP REM, F-29280 Plouzane, France.
[2] Univ Bretagne Occidentale, Lab Sci Environm Marin LEMAR, F-29280 Plouzane, France.
[3] Rudjer Boskovic Inst, LPCT, Zagreb 10002, Croatia.
[4] IFREMER, Lab Detect Capteurs & Mesures LDCM RDT REM, F-29280 Plouzane, France.
[5] IFREMER, Lab Cycles Geochim & Ressources LCG GM REM, F-29280 Plouzane, France.

* Corresponding author : Laura Cotte, email address : cottelaura@yahoo.fr

Abstract :

Environmental contextCopper released by deep-sea hydrothermal vents has been recognised to be partly stabilised against precipitation by its complexation with strong Cu binding ligands. Yet, the sources and nature of these compounds in such environments are still not fully understood. This study shows that the Cu ligands detected are hydrothermally sourced and could be mainly inorganic sulfur species. AbstractThe apparent speciation of Cu in the early buoyant plume of two black smokers (Aisics and Y3) from the hydrothermal vent field Lucky Strike (Mid-Atlantic Ridge) was investigated using competitive ligand exchange-adsorptive cathodic stripping voltammetry (CLE-AdCSV). We have assessed the apparent Cu-binding ligand concentration ([L]) and the corresponding conditional stability constant (log K) for 24 samples. At the smoker Aisics, [L] ranged from 18.2 to 2970nM. Log K-CuL ranged from 12.4 to 13.4. At Y3, the binding capacity of natural ligands was from 32.5 to 1020nM, with Log K-CuL ranging from 12.5 to 13.1. Total dissolved Cu ranged from 7.0 to 770nM and from 12.7 to 409nM at Aisics and Y3, respectively. Our results show that the amount of ligand L increases with dissolved Mn (dMn) concentrations, suggesting a hydrothermal origin of the Cu-binding ligands detected. In addition, such high concentrations of Cu-binding ligands can only be explained by an additional abiotic source differing from organic processes. Based on the massive in situ concentrations of free sulfides (up to 300 mu M) and on the striking similarities between our log K-CuL and the log K-Cu(HS) previously published, we infer that the Cu-binding ligands could be predominantly inorganic sulfur species in the early buoyant plume of the two vent sites studied.

1. Introduction

Speciation studies are crucial for understanding the biogeochemical cycle of trace metals in the open ocean. Commonly used to predict the biological availability and the toxicity of metals on microorganisms [1], chemical speciation also brings new insights on which chemical species are controlling the fate of a particular metal in a specific environment.

Hydrothermal fluids are the results of the leaching of oceanic crustal basalts by hot and acidic percolated seawater through the seafloor [2]; as a consequence, they are enriched in various inorganic [3] and in small amount of organic species [4,5]. The plumes discharging to the deep ocean are a complex mixture of dissolved and particulate species [3,6], mostly reduced, which concentrations depend on the extent of the basalt alteration (i.e. water/rock interactions), as well as the proportion of subsurface mixing with seawater [7]. Initial concentrations of species in the plume are also impacted by chemical reactions occurring throughout the mixing of the hydrothermal fluid with seawater.

Despite this complex mixture, previous speciation studies have emphasized the ability of inorganic sulfides to reduce the toxicity of divalent iron [8] or copper [9] by forming metal-sulfide complexes. These previous findings suggest that inorganic sulfides contribute to metal-complexation in hydrothermal vents. More recently, dissolved copper from deep-sea hydrothermal vents [10,11] and from shallow hydrothermal sources [12] has been recognized to be partly stabilized against precipitation by its complexation with strong organic chelates. These organic ligands, probably thiols [10], have been assumed to compete against inorganic sulfide complexation, hence preventing a part of Cu from being precipitated across the mixing with seawater. Model simulations have even shown that such organic compounds likely increase the solubility of copper, impacting thus the global Cu-fluxes in the ocean [13]. Specific organic ligands for iron have also been detected in hydrothermal buoyant plumes [14–16], suggesting a stabilization in the dissolved phase as well as a higher solubility of iron in the deep ocean.

However, the source and nature of these organic compounds in such environments are still poorly known. Organosulfur compounds coming from biologically-rich diffuse areas, rather than typical oceanic ligands (e.g. humic substances [17]) have been suggested to be the main organic species found in such environment and thus to represent these organic ligands [10–12]. Despite these assumptions, the potential impact of reduced sulfur species on metal speciation is still pointed out [11,12]. Because of their massive concentrations in the hydrothermal end-members (from µM to mM levels) [11,15], inorganic sulfides should indeed play an important role in metal-complexation in the early buoyant plume.

In this study we provide new data on the apparent speciation of Cu in the early buoyant plume of two black smokers located in the Lucky Strike hydrothermal vent field (Mid-Atlantic Ridge). We discuss the apparent ligand concentrations obtained in line with DOC levels and, for the first time, with the *in situ* measurements of total inorganic sulfides in the buoyant plume. We then anticipate on what is the nature of the copper binding ligands in the studied area in line with the corresponding *in situ* parameters measured.

2. Experimental

2.1. Sampling sites

Hydrothermal fluid samples were collected at the Lucky Strike vent field (37°N) during two oceanographic cruises on the RV Pourquoi Pas? and the Atalante (Momarsat 2015: http://dx.doi.org/10.17600/15000200 and Momarsat 2016: http://dx.doi.org/10.17600/16001200).

The Lucky Strike Seamount is located southwest of the Azores Islands on the slow-spreading Mid-Atlantic ridge (MAR) (~ 2.2 cm/yr [18,19]) and extends over almost 11 km at depth between 1800 and 2000 m [20]. The volcano summit is made of three volcanic cones surrounding a flat depression which hosts a fossil lava lake as well as the Lucky Strike vent field (average depth:

1690 m). Hydrothermal activity is gathered around the lava lake which prevents hydrothermal fluids from directly discharging through the crust [20–22]. The Lucky Strike vent field displays a wide variety of emission and structures which are all hosted on a basaltic substratum [23]. Two black smokers from Lucky Strike were selected to study the nature of the Cu-binding ligands: Aisics (32°17.34'N; 32°16.53'W, 1690 m depth) and Y3 (37°17.51'N; 32°16.67'W, 1726 m depth) (Figure 1).

2.2. Sampling method

At each site, *in-situ* filtration was carried out in the early buoyant plume of each smoker using the PEPITO sampler [24] implemented on the ROV Victor 6000 (Figure 1). Prior to use, all equipment used for sampling and filtration was rigorously washed with diluted hydrochloric acid (pH 2, Suprapur, Merck) and rinsed with ultrapure water (Milli-Q element system). The *in-situ* filtered samples were collected by pumping water into 2L-PVC/DEHP blood bags (Terumo, sterile treated by ethylene oxide, PVC/DEHP, 1BDT200BM) with on-line filtration at 0.45 µm (HATF, Millipore). For each dive, sampling was performed towards increasing temperatures, i.e. from the seawater-dominated to the hydrothermal-dominated part of the mixing zone, thus minimizing potential contamination of the sampler. The acid-cleaned titanium-silicone nozzle of the sampling device was first positioned in the buoyant plume, at 1 to 2 m from the vent orifice. A high-temperature probe coupled to the nozzle was used to monitor the temperature at each point of the mixing gradient sampled. When the temperature probe was stabilized at 4°C (coldest part of the mixing), the pumping of the first sample (A1) was started and held for 3 to 5 min. The nozzle was then shifted downwards within the central part of the buoyant plume with temperature increments of ~ 10°C until reaching values ranging from 100 to 150°C. Overall, 15 samples were collected for each of the 2 mixing gradients sampled. Pumping was systematically stopped in case of a steep increase in temperature (e.g.

10°C to 100°C in a few seconds) or a chimney structure collapsing to avoid samples contamination by particles.

Coupled to the PEPITO sampling, one chemical miniaturized analyzer (CHEMINI [25]) was used for the *in situ* measurement of sulfides ($\Sigma S = HS^- + S^{2-} + H_2S$) [26]. Briefly, ΣS measurement is based on flow injection analysis with colorimetric detection (methylene blue method). The chemical analyzer was calibrated *in situ* at the beginning and at the end of each dive using S(-II) stock solutions. Hydrothermal solutions were directly pumped without any filtration and the signal acquisition (~ 3 min) was initiated at the same time as the PEPITO sampling (the same titanium-Silicon cannula is used for both PEPITO and CHEMINI). The chemical species analyzed corresponded to an operationally defined fraction of sulfides, herein called free sulfides. This fraction included the dissolved and particulate sulfides in unfiltered seawater that are labile enough to react with methylene blue at pH 4.7 (acetate buffer). *In situ* measurement of dissolved oxygen was performed using an optode (Aanderaa).

Immediately after recovery of the ROV, samples were processed in the chemical lab on board (clean lab, Class 100 000, ISO 8) and pH was measured on dedicated aliquots using a daily-calibrated pH-meter (NBS buffers: pH 4, 7 and 10 at 25°C). Each bag was then sub-sampled for further spectrometric analysis of the total dissolved concentrations of dissolved manganese (dMn). Aliquots were stored in acid-cleaned 15 mL-polypropylene tubes (Elkay) and immediately frozen at -4°C until on shore analysis. The remaining volume in the PVC/DEHP-bags was dedicated to Cu-speciation measurements.

2.3. Storage strategy and analyses performed for the assessment of Cu speciation

The protocol used for storage and on-shore analyses for the assessment of Cu speciation is summarized in Figure 2. In total, thirty hydrothermal samples were dedicated to the study of Cu-binding ligands. Samples collected in 2015 were poisoned directly inside the PVC/DEHP-bag with sodium azide (NaN_3, extra pure, Merck) and stored at 4°C for one year. For 500 mL

of sample, a volume of 150 µL of NaN_3 (0.2 M) was added. It should be mentioned that both frozen and poisoned samples were available in 2015, with the aim at comparing the effect of sampling storage on Cu-speciation measurements (Figure 1). Though no comparative study was done yet, we chose the poisoning method because we suspected freezing to worsen aggregation of colloidal phases (black precipitates were regularly seen inside frozen bags). In addition, freezing at -20°C was reported to modify the original speciation of Cu, suggesting that this storage was not fully adapted for such measurements compared to a storage at 4°C [27]. However, storage of our samples (4°C) was longer (1 year), meaning that changes in speciation can occur before Cu titration analyses and that the results obtained for this year should be discussed cautiously. Samples from the second cruise (2016) were immediately transferred in 500 mL PFA bottles after recovery on board and also poisoned with azide before storage at 4°C for 2 months. Aliquots from bags and bottles were then analyzed on shore by High Resolution Inductively Coupled Plasma Mass Spectrometry (HR ICP-MS) for total dissolved copper (dCu) concentrations (see paragraph 2.5).

Reduced Sulfide Species (RSS) concentrations appeared to be so high in 2016 that a pretreatment of samples was needed to enable any electrochemical measurement of labile Cu. Prior to the complexometric titration experiments, samples were purged with clean air for about 1.5 h to remove volatile sulfides. They were left to equilibrate overnight and then filtered at 0.2 µm. Samples were not acidified before purging to minimize the chemical changes of the natural inorganic and organic ligands. We also tested the procedure which involves acidification of sample and purging with N_2, as described by Sander et al. [10], but we did not observe any improvement in the voltammogram shape when compared to the 'air purging' method we applied. The clean air purging led to the oxidization of some inorganic RSS as SO_4^{2-} but also as S^0 or polysulfides particles that probably trapped some dissolved Cu. To ensure a correct measurement of the remaining dissolved Cu, pretreated samples were re-analyzed by ASV as

150 described in section 2.4.2.d. The final Cu concentrations obtained for pretreated samples are
151 labelled dCu^* and are used for calculations of L^* concentrations and of $\log K'^*_{CuL}$. L^* and
152 $\log K'^*_{CuL}$ will thus represent the complexing parameters for Cu-binding ligand resistant to
153 oxidation processes. The pre-treatment was not required for samples from 2015 because of the
154 lower apparent RSS concentrations. Dissolved copper concentrations (dCu) obtained by HR
155 ICP-MS were used for calculations of L and $\log K'_{CuL}$. For voltammetric titration experiments,
156 untreated samples refer to samples collected at Y3 and Aisics in 2015.
157 Because samples collected in 2016 were treated differently than those collected in 2015, the
158 two datasets could not be directly compared. Despite this important issue, each dataset enabled
159 to shed different insights on the speciation of Cu in hydrothermal vents and was thus used
160 accordingly. On one hand, samples from 2015, which remained untreated, were the most
161 comparable to the other Cu speciation data that have been previously published. This dataset
162 was also the most reflective of relatively unperturbed Cu speciation, bearing in mind that any
163 hydrothermal sample is perturbed during storage or pH buffering. On the other hand, samples
164 from 2016 enabled to discuss on the relative importance of organic ligands relative to inorganic
165 ligands.
166

167 ## 2.4. Voltammetric measurements

168 ### 2.4.1. Analytical equipment and reagents

169 Voltammetric measurements were performed using the potentiostat-galvanostats
170 PGSTAT128N or μAutolab III (Metrohm) controlled by GPES 4.9 software coupled with a
171 three-electrode system 663 VA stand (Metrohm) at the Ruđer Bošković Institute (RBI),
172 Croatia. The working electrode was a Hanging Mercury Drop Electrode (HDME) (drop area:
173 0.25 mm^2). A double junction Ag/AgCl/sat. NaCl/UVSW and a platinum wire were used as the
174 reference and the counter electrodes, respectively. UVSW used for experiments refers to UV-

irradiated seawater collected off-shore of Šibenik (Croatia). Solutions were stirred during the deposition step by a quartz or a Teflon stirrer rotating at 3000 rpm. Experiments were conducted in a quartz cell with a working volume of 10 mL. All measurements were carried out at room temperature (~25°C). pH was monitored using a pH-meter (Orion Research, model 920) with a daily calibrated pH electrode (Metrohm). Ultra clean water (ASTM Type I, 18.2 MΩ; Milli-Q) used for final washings and preparation of chemicals was purified by combining Elix 5 and Synthesis 10 purification systems from Millipore. All sample containers were acid-cleaned with 10% nitric acid (HNO_3 65%, analytical reagent grade) and thoroughly rinsed with Milli-Q water before use. Only fluorinated ethylene propylene (FEP) or perfluoroalkoxy (PFA) bottles were used. Prior to voltammetric measurement, an aqueous stock solution containing 0.05 M salicylaldoxime (SA, 98% Sigma) was prepared and stored at 4°C. A 1 mM SA standard was then prepared from the 0.05 M stock solution and used for voltammetric analyses. A pH buffer was made by dissolution of boric acid (Suprapur, Merck) in 0.35 M ammonia (> 25%, TraceSelect, Fluka) to obtain a 1 M solution. The addition of 100 µL of this buffer in 10 mL sample gave a pH of 8.2 in the cell. Slightly acidic Cu standards solutions (10^{-6}; 10^{-5} and 10^{-4} M) were prepared in Milli-Q water (pH ~ 3) from a 1 $g.L^{-1}$ Cu-stock solution (Fluka).

2.4.2. Determination of Cu complexing parameters by CLE-AdCSV

2.4.2.a Titration procedure

The Cu binding ligands concentration ([L] or [L^*]) and the corresponding conditional stability constant (log K' or log $K'^{*)}$ were assessed using Competitive Ligand Exchange – Adsorptive Cathodic Stripping Voltammetry (CLE – AdCSV) with SA as the competing ligand [28]. Theoretical background as well as details for the calculation of complexation parameters are provided in supplementary information. In order to perform CLE-AdCSV experiments within

199 the linear range of the method (up to ~400 nM of Cu_T), untreated samples with high Cu content
200 (1st set) were generally diluted 10-fold in clean UVSW (dCu < 1 nM). Pretreated samples (2nd
201 set) were not diluted as the signal measured without addition of Cu was generally low.
202 Preparations for titration experiments were carried out under a laminar flow hood in a 500 mL-
203 acid-cleaned FEP bottle and in fifteen 30-mL acid-cleaned FEP flasks with ETFE screw caps.
204 A 16th 30-mL flask was used for the blank. The analysis was carried out using an automated
205 system equipped with an in-house made sample changer which allowed the addition of the
206 sample in the cell plus a rinse between each aliquot. A volume of 20 mL was needed in each of
207 the 15 flasks (i.e. 10 mL for the rinse and 10 mL for the analysis). When 10-fold diluted, 30 mL
208 of sample was first transferred in the 500-mL FEP bottle. Then, borate buffer and SA were
209 added in order to reach a pH of 8.2 ± 0.2 and a SA concentration of 4 µM in final solution.
210 UVSW was finally added to achieve the total volume of 300 mL. 20 mL aliquots of the solution
211 were then pipetted into the 15 FEP flasks. Cu was added to each flask in logarithmic steps [29]
212 progressively increasing the additions from 0 to 300 nM by using automatic burette system
213 (XE1000, TECAN). The blank consisted of UVSW prepared directly in the 30-mL flask with
214 0.01 M borate buffer and 4 µM of SA. The 16 flasks were left to equilibrate overnight at room
215 temperature (8 h minimum). Concentration of labile Cu was then determined by CSV using
216 30 to 180 s deposition time. The deposition potential was -0.1 V followed by a 5 s equilibration
217 time and a cathodic scan from 0.05 V to -1.6 V using the square wave (SW) mode (step potential
218 2 mV, frequency 50 Hz). Five repetitions for each aliquot were made for quality control.
219 Overall, precision was better than 2%. The titration experiment performed in UVSW showed
220 fully linear response, confirming that the chosen titration range was adequate.
221 Once the voltammogram treatment was performed (see 2.4.2.c), final titration curves were
222 plotted in the ProMCC software. Conditional stability constant as well as ligand concentrations
223 were modelled using the complete complexation-fitting model [30]. For all samples, the use of

1 ligand model gave proper estimations of both conditional stability constant and Cu-binding ligands concentrations.

2.4.2.b Side reaction coefficient

Most of samples were diluted in UVSW of salinity 38 resulting in a final salinity of around 35-36 in the measured samples. As salinity and the SRC of CuSA were close among samples, calculations of stability constants for diluted samples were all conducted with a salinity value of 36. Values of 9.54 and 14.96 for log K'_{CuSA} and log $\beta'_{Cu(SA)2}$ were obtained and used for all further calculations. A value of 13 was chosen for inorganic side reaction coefficient α_X and used in calculations [31].

2.4.2.c Signal treatment and final titration curves

All voltammograms treatment was performed using the software ECDSOFT available at https://sites.google.com/site/daromasoft/home/ecdsoft [32]. Raw signals were first corrected from noise using automatic smoothing (Savistky-Golay method [33]). Smoothed voltammograms were then automatically subtracted by the blank (which was flat in the potential range of $Cu(SA)_x$ peak). Additionally, the baseline at the position of $Cu(SA)_x$ peak was manually subtracted for each voltammogram using the 'spline' procedure [34]. The reduction peak corresponding to the $Cu(SA)_x$ complexes was found at ~ 0.35 V (Figure 3). A 'shoulder' was also observed on the positive side of the main Cu-SA peak and could be linked to other Cu-complexes existing in the sample, such as Cu-sulfides nanoparticles [35–37].

2.4.2.d Total dissolved Cu in pretreated samples

Total dissolved Cu concentration in pretreated samples (dCu^*) was determined using differential pulse anodic stripping voltammetry (DPASV). Prior to analysis, 10 to 20 mL of hydrothermal fluid samples were acidified to pH < 2 (20 to 40 µL of HNO_3 69 %, Suprapur) and then UV-irradiated overnight (250 W high pressure mercury lamp). Electrochemical paramaters were adapted from Omanović et al. [38]. Samples were first deaerated by purging the solution for at least 5 min. The accumulation was performed at a deposition potential of -1 V for 120 or 180 s, followed by an anodic stripping scan from -0.45 to 0 V using the differential pulse (DP) mode (modulation time 40 ms, modulation amplitude 40 mV, step potential 2 mV and interval time 0.1 s). A 2-s potential-jump to -1.3 V was applied at the end of the accumulation time. This step is needed for non-UV irradiated samples at natural pH in order to desorb any layer of natural organic matter from the mercury drop [39], but was also found to slightly improve the baseline shape in acidic and UV-irradiated samples. The equilibration time was set to 5 s. Cu concentration was determined using the standard addition method. Every measurement was repeated 3 times for quality control.

2.5. Total dissolved Cu and Mn concentrations in untreated samples

Untreated samples (both sets) were analyzed by HR ICP-MS (Element 2, Thermo Finnigan; at IRB, Zagreb) and by ICP-AES (Ultima 2, Horiba Jobin Yvon; at PSO, Brest) for dCu and dMn concentrations, respectively. The measurement of dCu concentrations was performed after dilution of the samples from bags and PFA-bottles in a 2% HNO_3 solution (dilution factor: 10) spiked with a stock solution of indium (1 $g.L^{-1}$) as internal standard (final concentration: 10 $\mu g.L^{-1}$). External standards of Cu were then prepared in the matrix matching media (UWSV, 2% HNO_3) for the assessment of dCu. The analysis of dMn was conducted on aliquots stored

in 15 mL pre-cleaned polypropylene tubes (Elkay) dedicated for ICP measurements. Preparation of solutions and standards is more detailed in Cotte et al. [40]. Blanks included several replicates of the 2% HNO_3 solution as well as ultrapure water processed in the PEPITO sampler. Repeatability (n = 10) was 3% for dMn and 4% for dCu. Dissolved concentrations presented here were generally well above the detection limits. Blanks were below detection limits and mostly negligible when compared to dissolved concentrations. It should be mentioned that acidification alone in sulfidic waters has been previously reported to result in a significant underestimation of total dissolved Cu because of the formation of stable Cu sulfide phases which can adsorb onto bottle walls [41]. However, overlooking total dCu concentrations is much more critical for the correct interpretation of the dCu spatial distribution in relation to the hydrothermal vent distance, than for the complexation study by which we tried to identify possible ligands (organic/sulfur derived) which control Cu speciation. Due to the complexity of such studies, including sample collection, preservation, storage and, finally, measurement, it is certain that some absolute values (e.g. concentrations of dCu) do not correspond to the ambient conditions. However, the observed experimental/voltammetric phenomena are supposed to be mostly unaffected regardless of the total concentrations of some compounds.

2.6. Dissolved organic carbon

Samples were pipetted in glass tubes cleaned with 10% HNO_3 (analytical reagent grade), rinsed with Milli-Q water and calcinated for 4 hours at 450°C. Dissolved organic carbon (DOC) measurement was conducted by direct injection of the sample into the furnace for combustion at a temperature of 680°C through a highly sensitive catalyst (Pt) [42]. Formed CO_2 was then measured by a non-dispersive infrared analyzer (NDIR). Dissolved inorganic carbon (DIC) was removed from the solution by acidification of each sample with a 2% HCl solution to pH 2-3 and bubbling with clean air stream for 10 min. Calibration was performed using potassium

hydrogenophtalate as a standard. Sample from each cuvette was measured in triplicate and standard deviation was calculated (0.01 mg.L^{-1}). Note that DOC was only measured on the 2016 samples.

3. Results and discussion

3.1. Master variables

All Cu speciation parameters and the associated master variables measured in the present study are summarized in Table 1, Table 2 and Table 3. Dissolved manganese (dMn) was used as conservative tracer because of its well-known very slow scavenging rate in the plume [43,44]. As expected, samples from the early buoyant plume were highly enriched in dMn at both sampling sites compared to typical deep-seawater concentrations (dMn ~ 0.5 nM at 1700 m depth [45]). The 3 sets of samples collected at Aisics (2015 and 2016) and Y3 (2015) displayed dMn concentrations ranging from 1 to ~ 100 µM indicating that the examined area corresponds to a dilution of the hydrothermal solution with local seawater of ~ 3 to ~ 300 (Table S1). In addition, similar T–dMn linear relationships were observed at both vent sites (T ~ 1.5dMn).

Dissolved Cu concentrations (dCu) in untreated samples were generally found in the range 10-800 nM at both vent sites with values from 12 to 771 nM and from 13 to 409 nM at Aisics and Y3, respectively (Table 1). This is much higher (one or two orders of magnitude) than the ambient concentrations reported in deep-seawater of the North Atlantic (2–3 nM [46,47]) but typical of hydrothermal input. As opposed to dMn, concentrations for dCu differed between the two vent sites, Y3 displaying globally higher dCu concentrations than Aisics (dCu = 5.6dMn vs. dCu = 3.0dMn, respectively). This discrepancy suggests different physico-chemical properties in the corresponding end-members fluids (e.g. higher dCu at Y3). Note that at Aisics,

317 a low year-to-year variability of dCu in the mixing gradient was observed for the 2 sampling
318 years (Table 1 and Table 2).
319 In pretreated samples, dissolved Cu concentrations (dCu^*) were much lower than the original
320 dCu. Indeed, dCu^* at Aisics varied between 2.5 and 14 nM whereas corresponding dCu ranged
321 from 7 to 410 nM (Table 2). Such difference arises from the removal of the dCu by adsorption
322 onto the PFA bottle walls over the storage period and by additional scavenging onto the newly-
323 formed particles resulting from the air-purging treatment.
324

325 ### 3.2. *In situ* concentrations of sulfides and oxygen

326 Concentrations of *in situ* free sulfides ($\Sigma S = HS^- + S^{2-} + H_2S$) and dissolved oxygen are
327 summarized in Table 3. *In situ* concentrations of ΣS ranged from 1 to 320 µM and from 5 to
328 350 µM at Aisics in 2015 (dive 02598) and in 2016 (dive 09632), respectively. The ΣS
329 concentrations were slightly higher at Y3 as they were ranging from 52 to 415 µM. Like for
330 dCu, this difference could be due to a different chemical signature of each end-member fluid.
331 Note that the ΣS data were not measured in 2015 at Y3. We thus chose to use the ΣS data
332 measured in 2014 at the same site. Such earlier data can be considered representative of free
333 sulfide conditions occurring at Y3 considering the very low variability observed for other
334 chemical parameters at that site between 2014 and 2015 [48]. As expected, *in situ* ΣS levels were
335 increasing with dMn and T, towards the vent orifice (Figure 5, Figure 6 and Figure 7). Note
336 however the positive anomaly in ΣS observed at Aisics where ΣS concentrations reach more
337 than 300 µM at around 50 µM of dMn (Figure 5). Changes in the *in situ* dissolved oxygen (O_2)
338 levels along the mixing gradient were not as steep as it was noticed for ΣS. Concentrations were
339 indeed slowly decreasing with increasing dMn concentrations from 276 to 146 µM
340 (avg = 200 µM) and from 264 to 183 µM (avg = 230 µM) at Aisics and Y3, respectively (Table
341 3). The two vent sites generally displayed similar oxygen levels throughout the mixing gradient,

though slightly lower levels were sometimes found at Aisics (e.g. at dMn in the range 10–50 µM).

3.3. Description of the voltammograms

In our hydrothermal samples, voltammograms differed from those classically obtained in seawater because of the occurrence of interferences on the $Cu(SA)_x$ signal as well as several additional peaks. As their description can provide an 'imprint' of the hydrothermal environment, a complete scan from 0.05 to -1.6 V was performed during stripping. None of these interferences or additional peaks were detectable when analyzing UVSW, indicating a natural origin of the compounds involved and not an artifact from the method. In this section, we investigate on the nature of these additional peaks thanks to laboratory tests and literature. We then discuss on the interferences affecting the $Cu(SA)_x$ signal.

3.3.1. On the nature of additional peaks

Voltammograms for untreated and pretreated samples are presented in Figure 3. The peak at -1.45 V was related to the reduction of dMn (it is not accumulated) as the peak height was increasing in response to Mn(II) additions (Figure S1). As expected, the closer from the vent orifice, the higher was the dMn signal (Figure S2).

The massive signal observed at -0.6 V vs. Ag/AgCl in pretreated samples (Figure 3B) could be related to the high ambient reduced sulfur species (RSS) [49,50] in our samples, in line with the high *in situ* concentration of ΣS measured (up to 300 µM). The signal is much lower but still visible in untreated samples (Figure 3A). The peak likely corresponds to the dissolution-reduction of an HgS layer deposited on the mercury drop surface as reported in many studies [50–55]. Many sulfur species could contribute to the HgS layer deposition especially sulfides (HS^- and S^{2-}), but also dissolved elemental sulfur S^0 (< 0.2 µm), polysulfides (S_n^{2-}) [52,56] or metal

sulfide nanoparticles [35–37,57,58]. According to the excess of the *in situ* free sulfide concentrations measured, free sulfides should be the dominant RSS in our samples. In the experimental conditions used (pH ~ 8), HS^- might be the dominant free sulfide species and the formation of the insoluble HgS layer at deposition potential more positive than -0.5 V could therefore be expressed according to the following reversible two-electron process [49] (1):

$$HS^- + Hg^0 \leftrightarrow HgS_{layer} + H^+ + 2e^- \quad (1)$$

As dissolved Fe concentrations are relatively high in untreated samples (~2–200 µM [48]), we cannot exclude that some dissolved Fe would still persist as Fe(II) species, even after the pre-treatment. If so, the diffusion of labile Fe(II) to the Hg electrode may change the HgS layer formed with sulfides to a FeS layer [58] (2):

$$HgS_{layer} + Fe^{2+} + 2e^- \leftrightarrow FeS_{layer} + Hg^0 \quad (2)$$

FeS layers could also be generated by the direct deposition of FeS nanoparticles at the electrode surface [58]. Since the FeS layers deposited are re-dissolved at around -0.6 V [58], they could partly contribute to the massive signal observed in pre-treated samples. In addition to sulfide species, thiols could also contribute to the large peak observed, this compounds providing a peak at the same potential [59,60]. It is also important to underline that the height of the peak at -0.6 V was decreasing with additions of Cu (Figure 3B). This suggests that the specie(s) involved, i.e. sulfides or thiols, is(are) reacting with the added Cu throughout the titration experiment [50,60].

The peak at -0.1 V, which does not increase with the accumulation time, observable for both untreated and pretreated samples could be related to three different reduction processes (Figure

3). The first one could be iodide which was found to occur at that potential in estuarine samples, though easily removed through the application of a desorption step at more negative potential [17]. Unfortunately, neither the addition of potassium iodide in the buffered samples (pH 8.2, not shown), nor the application of the 1-s jumping potential did produce any increasing or removal of the peak of interest, respectively. Combined with the fact that iodide is not a major compound of hydrothermal fluid compared to chloride, this first hypothesis was thus excluded. Another possible explanation could be the deposition of a copper-sulfide layer on the drop surface as a result of an exchange reaction between Hg^{2+} from the HgS layer and labile Cu in solution, according to the reversible reaction (3) [55]:

$$HgS_{layer} + Cu^{2+} + 2e^{-} \leftrightarrow CuS_{layer} + Hg^{0} \quad (3)$$

Labile Cu could correspond to weak Cu-complexes or, potentially, Cu-sulfides nanoparticles (clusters). Such process has been shown to happen for many metal as Zn^{2+} or Fe^{2+} but only the formation of the CuS layer provides a signal at -0.1 V vs Ag/AgCl (e.g. E ~ -0.6 V for the FeS layer) [53,55]. Once deposited, the CuS layer will be reduced at ~ -1.0 V vs Ag/AgCl [35–37,55] as described in reaction (4) :

$$CuS_{layer} + H^{+} + 2e^{-} \rightarrow Cu^{0} + HS^{-} \quad (4)$$

Among voltammograms of untreated samples, this reduction peak was sometimes noticeable (up to 15 nA, Figure 3A). In pretreated samples, this signal was not observed, probably because hindered by the massive HgS reduction peak. The peak potential of the CuS formation process (3) is determined by the solubility product K_{sp} of CuS [55]. Through the titration experiment, K_{sp} will increase with increasing addition of Cu whereas pK_{sp} will decrease. Consequently, the peak

potential will be slightly shifted towards more negative potential as shown by Milanović et al. [55]. This feature was not observed when performing titrations, except some slight shifting of the presumed CuS peak toward more positive potential in few cases (Figure 3A). In addition with the potential shifting observed, the peak height was not dependent on the accumulation time. However, the peak height was increasing when getting closer to the vent source (Figure S2). This led us to the final assumption that the peak of interest could be related to thiosulfate, which is known to be formed in hydrothermal vents by the slow oxidization of sulfides [61]. Thiosulfate ($S_2O_3^{2-}$) reduction occurs at around -0.1 V vs Ag/AgCl and is well separated from the global sulfides reduction peak (-0.6 V) at pH 8 [51,52]. The interaction between thiosulfate and mercury results in the formation of a soluble complex via the oxidation of Hg according to the two electron process (5):

$$2S_2O_3^{2-} + Hg^0 \leftrightarrow [Hg(S_2O_3)_2]^{2-} + 2e^- \quad (5)$$

The soluble complex cannot be pre-concentrated to the drop surface as it immediately goes back to solution after its formation (as mentioned above, this peak does not increase with the accumulation time). The cathodic scan enables then to strip only the quantity of $[Hg(S_2O_3)_2]^{2-}$ formed on the drop surface at that precise moment, the current measured corresponding to the reduction of Hg^{2+} to Hg^0 [51]. Unfortunately, addition of sodium thiosulfate was not performed on samples to confirm this assumption. Besides, the aforementioned studies were working on laboratory solutions with known concentrations of all species in solution or on samples not truly representative of hydrothermal samples. Accordingly, the identification of each electroactive species in such unusual samples must be more problematic and more tests should be further carried out to decide which process is truly happening. Hence, the peak at -0.1 V vs Ag/AgCl could be both related to the CuS layer formation and to the thiosulfate reduction.

3.3.2. Interferences on the $Cu(SA)_x$ signal

Interferences on the $Cu(SA)_x$ signal were observed in most of hydrothermal samples (Figure 3). At low addition of Cu, unknown peak/shoulder at ~ -0.27 V was systematically overlapping with the $Cu(SA)_x$ signal in both untreated and pretreated samples. A similar shoulder is observable in voltammograms presented on the 'Figure 1.b' of Sander et al.'s paper [10]. In both datasets, the corresponding reduction signal was thus fitted and de-convolved from the interferences observed at ~ -0.27 V using the ECDSOFT program. Depending on the sample, 1 or 2 peaks were considered to overlap with the main $Cu(SA)_x$ reduction peak. Signal de-convolution was performed by starting from the signal corresponding to the highest Cu addition, where interferences no longer overlook the $Cu(SA)_x$ reduction peak, towards the signal corresponding to the lowest Cu addition, where extraction was more liable to errors. The height of the de-convolved peak of $Cu(SA)_x$ was then measured and used to construct the final titration curves which consist in the relationship between the measured current (i_p) and the total concentration of Cu (Figure 4).

Note that the $Cu(SA)_x$ signal at ~ -0.3 V obtained for pretreated samples was not well defined, especially at low additions of Cu where it appears flattened and narrower compared to the one observed in untreated samples (see boxed window (*), Figure 3B). The spike observed did not correspond to a reversible process which suggest that it was not related to the reduction of the $Cu(SA)_x$ complex. With increasing additions of Cu, the spike was shifting towards more positive potential (-0.27 V) until the appearance of a second peak corresponding to the reversible reduction of the $Cu(SA)_x$ complexes at -0.3 V. In addition, the maximum reduction current for the $Cu(SA)_x$ signal, corresponding to the last addition of Cu (same final concentration), was ~ 200 nA in pretreated samples whereas it reached almost 400 nA for

460 untreated samples. These issues are likely related to the HgS layer formed at the mercury drop.
461 By occupying most of the space available on the drop, the HgS layer probably prevents the
462 $Cu(SA)_x$ complexes from adsorbing on the drop surface. This feature has already been observed
463 by Powell [11] who mentioned both an over-scale reduction peak at -0.5 V (vs Ag/AgCl) related
464 to RSS and a poorly defined $Cu(SA)_x$ peak, but before any pre-treatment of his hydrothermal
465 samples. Consequently, the HgS layer formation as well as its reduction are interfering on the
466 $Cu(SA)_x$ signal, although the two reduction peaks are not overlapping.
467 In an attempt to remove the HgS interference, a 1-s potential-jump to -0.65 V to desorb the HgS
468 layer from the drop was performed to the air-purged samples at the end of the accumulation
469 step. This desorption step effectively removed > 95% of the HgS interference. However,
470 comparative experiments in model and real samples showed that this procedure is providing
471 good results on model samples whereas its application on real hydrothermal samples still needs
472 to be more explored, because of problems with the linearity. Though unsuccessful, the
473 procedure employed is described in supplementary information. Note that the HgS interference
474 should also be high in untreated samples since the *in situ* concentrations of ΣS are similar than
475 for pretreated samples. It was not the case because untreated samples were 10-fold diluted and
476 were analyzed a year after collection, meaning that most of the free RSS could have been slowly
477 oxidized with time by O_2 excess in samples (e.g. ~ 200 µM, Figure 5) or potentially by slight
478 air passing through sampling bags. By contrary, pretreated aliquots were analyzed only 2
479 months after sampling, meaning that a short time is required between sampling and
480 electrochemical analysis for speciation studies. In conclusion, fairly good titration curves were
481 obtained from the classical analysis used for speciation studies [28] but titration of the Cu-
482 binding ligands was more problematic than expected in 2016 because of the high ambient sulfur
483 species. Despite not fully identified, sulfur species obviously play a major role in the early
484 buoyant plume and likely interfere on Cu speciation measurement in this area.

485

486 ### 3.4. Cu-complexing ligand parameters

487 Concentrations for Cu-binding ligands ([L]) in the untreated samples ranged from 0.032 to
488 3 µM (avg. 700 nM, n = 19; Table 1). Aisics and Y3 both exhibited similar concentrations for
489 [L] which varied between 0.23 and 3 µM and from 0.032 to 1 µM, respectively. Interestingly,
490 an increasing trend towards the plume core clearly appears when plotting both [L] and ΣS
491 against the dMn concentrations at Y3 (Figure 6). This suggests a common source for all these
492 parameters including the Cu-binding ligands. This feature has already been observed close to
493 deep-sea vents for Fe-binding ligands which were highly correlated with the hydrothermally
494 sourced Fe concentrations ($r^2 = 0.996$) [16]. The trend was less clear at Aisics where [L] were
495 globally flattened by two samples displaying the highest concentrations measured (02598 B1
496 and 02598 D3) (Figure 5). Note that the corresponding dCu concentrations in these two samples
497 were also the highest measured (770 and 460 nM, resp.), indicating that these two exceptions
498 for [L] were not an artefact from the titration experiments. However, it should be mentioned
499 that, when these two 'outliers' are not considered, a very good match between [L] and the
500 anomaly of ΣS is observed (not shown). Stability constants ($\log K'_{CuL}$) remained globally
501 similar at both sites: calculations provided $\log K'_{CuL}$ values ranging from 12.37 to 13.38
502 (avg. 12.89).
503 To our knowledge, Sander et al. [10] and Klevenz et al. [62] are the only studies for which titration
504 experiments have been conducted on untreated hydrothermal samples (i.e. non-acidified, non-
505 purged) and thus to which our results for L can be directly compared. Our untreated samples
506 displayed [L] in similar range than concentrations previously measured at the Kermadec Arc in
507 Pacific [10]. The authors have indeed reported concentrations for Cu-binding ligands ranging
508 from 125 nM to 4.5 µM (avg. 1.7 µM, n = 4). However, Klevenz et al. [62] have reported
509 narrower concentration ranges (50 - 200 nM) from diffuse hydrothermal fluids of the MAR,

with an average value of 125 nM (n = 2). Interestingly, our obtained stability constants (12.37–13.38, avg. 12.89 ± 0.11) are also very close to those observed by Sander et al. [10], i.e. log K'_{CuL} ranging from 12.53 to 13.46 (avg. 12.88 ± 0.61). A similar ligand class has therefore been measured in both cases, suggesting that the Cu-binding ligands found are likely to be of same nature. Although Sander and co-workers have attributed their findings to the occurrence of strong organic ligands (i.e. thiols), it is also worth mentioning that a log K'_{CuL} value of 12.9 has been found for Cu-bisulfide complexes using ligand competition with oxine at pH 8 [50]. Regarding their similar stability constants, both strong organic and inorganic bisulfide ligands could therefore be considered as part of the Cu-binding ligands mixture. It should be mentioned that both Cu(I) or Cu(II) species could be part of the Cu-complexes detected. The existence of Cu(I) is probable in hydrothermal samples because of the complex redox reactions in which Cu is involved [63]. The existing Cu(I) species could be further stabilized by complexation with thiols, as previously suggested [64,65]. In our case, the oxidation of Cu(I) during sample storage is likely to occur [66] and it would be too speculative to claim that the observed Cu speciation is mainly related to Cu(I)-thiol compounds. However, the formation of Cu(I)-thiol complexes should also be considered with specific experiment designed in order to prove such complexation scenario.

3.5. On the nature of dissolved copper ligands in the buoyant plume

Below, we discuss the potential sources of Cu-binding ligands (organic and/or inorganic) which could explain at best the high concentrations for L measured in our samples, in line with our available data set for DOC and for *in situ* free sulfides. We then consider copper speciation under laboratory conditions and discuss the implications deduced from [L^*] on the persistence of hydrothermal Cu-binding ligands in the oxic water column.

3.5.1. Organic Cu-ligands

DOC in deep ocean waters is mainly composed of refractory organic matter originally coming from sea surface [67] and resistant enough to removal processes such as microbial activity. In deep waters, background concentrations of refractory DOC are averaging 45 µM [68,69] whereas concentrations detected in focused and diffuse vents range on average from 15 to ~ 100 µM [70,71] and from 50 to ~ 100 µM [70–72], respectively. The oldest (or most refractory) forms of the deep DOC pool are almost all removed (> 90%) through thermal degradation in subseafloor circulation [71,73] but, still bulk DOC concentrations remain important because of carbon-rich sediment remobilization as well as local input of abiotically-produced organics compounds [4,71].

Our samples display DOC concentrations ranging from 25 to 90 µM (avg. 53 µM) which is slightly above background DOC in deep seawater (45 µM) but in the range of previous finding in hydrothermal vents. The highest value corresponded to one of the closest sample from the vent source (09632 C3) (Table 2) though no particular trend has been noticed along the mixing gradient. In surrounding deep Atlantic waters, concentrations of organic ligands have been reported to be in the range of 2-4 nM [47]. So, basically, organic ligands from deep seawater account for 0.01% of the deep recalcitrant DOC pool. More importantly, those organic ligands can only provide a very limited part of the Cu-binding ligands observed here (up to 3 µM). A deep local source must therefore explain the enhanced concentrations measured for L.

First, organic compounds including organosulfur Cu-ligands could be directly produced in the hydrothermal fluid, before venting [74]. Synthesis of thiols through abiotic reduction of the hydrothermally-sourced inorganic carbon (CO_2 or CO) has indeed been suggested for H_2-rich fluids [75]. However, this process has been reported to be limited. In addition, the hydrothermal fluids from Lucky Strike show relatively low levels in H_2 when compared to other sites from

559 the MAR such as Rainbow [76]. Instead, thermal degradation of microbial communities with the
560 associated dissolved organic matter in subsurface has been suggested to produce methanethiols.
561 The abundance of such specific compounds has been reported to be around 10 nM in high
562 temperature fluids (> 200°C) [4]. Indeed, the authors have performed measurements of
563 methanethiols in the end-members fluids of 4 smokers located in the Lucky Strike vent field.
564 The resulting concentrations were around 6–7 nM with a maximum of 23 nM (avg. 10 nM).
565 Since the Aisics and Y3 end-members both display temperatures greater than 300°C (Table S1),
566 the abundance of methanethiols are likely to be in a similar range, i.e. lower than 20 nM.
567 Second, organosulfur ligands with available binding sites could be supplied by microbial
568 production in diffuse areas. If located in the close vicinity of focused black smokers
569 (e.g. Aisics), then microbially-produced ligands could be laterally entrained in the buoyant
570 plume, as suggested for larvae [77]. Cultured microbes from two hydrothermal vents of the MAR
571 have indeed been reported to produce organic Cu-binding ligands as a protection against the
572 enhanced Cu concentrations [62]. In response to the addition of 100 nM of Cu, around 200 nM
573 of Cu-binding ligands were produced in one of the cultures, which is not negligible but still not
574 completely explaining the enhanced level for L in the present study.
575 Finally, laterally entrained microbial communities could produce organics directly in the early
576 buoyant plume, where temperature falls down rapidly under 100°C. However, we anticipate
577 that the early mixing of the studied gradients (on the order of ten seconds) should be much
578 faster than microbial production of organic compounds. Although not known for hydrothermal
579 microbes, the kinetic of production for organic ligands by phytoplankton in response to metal
580 enrichments has been found to be around 1 nM per day for specific zinc-binding compounds
581 [78], which is much longer than the mixing time.
582 Overall, deep local sources of potential organic Cu-ligands are existing in deep-sea
583 hydrothermal vents but the input appears to be relatively limited and can only explain a small

584 part of the Cu-binding ligands measured in the buoyant plume. As none carbon-rich sediment
585 remobilization has been noticed during sampling – the lava lake is moderately covered by
586 sediment [20] – other sources as well as other type of ligands should be considered such as the
587 input of inorganic Cu-binding ligands by vent sources. It is worth noting however, that the
588 fraction of Cu-ligands resistant to the air purging treatment (L^*) could correspond to organic
589 species. Their concentrations, up to 20 fold lower than those of the ligands L (range 18–44 nM;
590 Table 2) appear to be on the same order of magnitude than the aforementioned potential organic
591 sources. Their stability constants (log K'^{*}_{CuL}) range from 12.57 to 13.04 (avg. 12.79) and are
592 thus comparable to those found for thiols [10,60]. When plotting [L^*] against dMn at Aisics
593 (Figure 7), the highest concentrations for L^* were observed closer to the hydrothermal end-
594 member, at dMn concentrations about 75 nM (corresponding to a temperature of ~ 120°C). This
595 feature suggests that the ligands L^* are hydrothermally sourced. Nevertheless, more samples
596 would have been needed in the hotter part of the mixing to confirm this assumption.
597
598 **3.5.2. Inorganic Cu-ligands**
599 Chloride and sulfides are recognized to be the dominant inorganic Cu-binding ligands in
600 hydrothermal fluids [9,79]. While Cu(I)-chloride complexes dominate in hot (~ 300°C) and acidic
601 (pH < 3) fluids [80], Cu-sulfides complexes become predominant at temperature lower than
602 150°C with increasing pH [79]. Upon mixing with seawater, the temperature of hydrothermal
603 fluids rapidly falls down under 150°C leading to weaker Cu-chloride complexes. Cooling
604 promptly establishes a competition between chloride and sulfides for Cu and Cu-sulfides
605 complexes progressively overlook the Cu-chloride complexes [80].
606 Because of their high stability constant, comparable to that of strong organic ligands and their
607 massive concentrations measured *in situ* (> 100 µM) (Figure 5, Figure 6 and Figure 7), we infer
608 that inorganic sulfides could be the main contributors of the enhanced Cu-binding ligands

609 concentrations observed in the early mixing. This assumption is supported by the fact that the
610 log K'_{CuL} value we found at deep-sea vents were very similar to those reported by Al-Farawati
611 and van den Berg [50] for Cu(HS) complexes (i.e. 12.9). Moreover, the *in situ* concentrations of
612 inorganic sulfides are greater than 100 µM in most of our samples (Table 3). At such level of
613 inorganic sulfides, Al-Farawati and van den Berg have shown that the competition between
614 organic ligands and bisulfide for Cu does not exist anymore since the effect of organic
615 compounds on Cu-speciation becomes negligible when bisulfide concentrations are greater than
616 1 nM. The slow kinetics reported for the abiotic oxidation of sulfides by oxygen in diffuse
617 hydrothermal vents strengthen this hypothesis [61]. The authors have indeed calculated sulfides
618 oxidation rate lower than 1 $nM.min^{-1}$ which is negligible when compared to the mixing velocity
619 of the early buoyant plume (22-119 $cm.s^{-1}$ [81]) and to the total sulfides concentrations.
620 Furthermore, using *in situ* voltammetry, they did not find enhanced concentrations of sulfur
621 oxidation intermediate (i.e. thiosulfate or polysulfides), attesting to the slow oxidization process
622 of H_2S and HS^- in the mixing [61].
623 As pH is around 5 for all samples, the inorganic sulfide species should be mainly found as H_2S
624 and HS^-. With the progressive mixing with seawater, pH will gradually increase until 7–8, and
625 sulfides will be mostly found as bisulfides HS^-. Consequently, the inorganic Cu-sulfide
626 complexes should be mainly found as $Cu(HS)^+$ or as $Cu(HS)_2$ [50] and, in any case, should
627 largely overtake the organic ligands in the early mixing. Elemental sulfur S^0 could also interact
628 with the ambient Cu [11], though it is hard to know to which extent in the present study. However,
629 with the aging of the plume, local mixing of the plume with biologically rich diffuse vents
630 should lead to the input of organic ligands (e.g. thiols) which would mainly come from biotic
631 interactions. Such input would then increase the impact of organic ligands on the speciation of
632 Cu. We hypothesize that organosulfur compounds and stabilized sulfides (i.e. bound to Cu or

633 another metal) might coexist in the neutrally buoyant plume, until the complete oxidation of the
634 inorganic copper-sulfides complexes.

635

636 ### 3.6. Chemical changes of *in situ* speciation in laboratory conditions

637 As soon as samples are collected, free sulfides start going through progressive oxidation
638 because of the excess of O_2 in samples as well as some potential slight air-passing through the
639 bags/bottles. Despite this slow removal, our results show that free sulfides still control Cu
640 speciation at least 2 months after sampling. Facing such dominance, all previous studies aiming
641 at defining organic copper complexation in hydrothermal vents have performed an acidification
642 pre-treatment (pH < 2) followed by N_2-purging to remove any ambient RSS [82] in order to
643 measure only labile Cu released from the remaining organic ligands [10–12]. As mentioned
644 previously, we tested this protocol, but did not observe any difference in the voltammogram
645 shapes and final results.
646 In an attempt to distinguish the organic part from the ligand pool and to fasten the process of
647 sulfur species oxidation which already started inside of the PFA bottle, we simply air-purged
648 and re-filtered at 0.2 µm samples (2^{nd} set) for titrations of Cu-binding ligands. Lower Cu-
649 binding ligands concentrations were systematically found in these pretreated samples, attesting
650 that sulfides species removed are part of the Cu-ligands measured. On the contrary, air purging
651 would not have impacted organic ligands that much. Assuming that L^* mostly stand for organic
652 ligands, i.e. strong organosulfur ligands as thiols [10], the organic pool still constitute a limited
653 part of the global ligand pool found in untreated samples. Furthermore, L^* could also be used
654 as the utmost example to show how much Cu-complexes are resistant to strong and fast
655 oxidization. Note that the extent to which RSS were removed is unknown for both sets, but the
656 shape of voltammograms clearly show that these compounds still have an influence on Cu-

speciation, in accordance with the known stability of Cu-sulfides complexes in oxic conditions [82,83]. In deep waters, the mixture of Cu-binding ligands including organosulfur compounds and stabilized sulfides which results from the progressive mixing with seawater, is therefore able to cope with the rapid mixing between hydrothermal fluid and seawater which could enable dissolved Cu to be transported far from the venting source.

4. Conclusion

We assessed the apparent speciation of Cu in the early mixing with seawater of two different black smokers at the Lucky Strike hydrothermal vent field (Mid-Atlantic Ridge). The Cu binding ligand concentrations were increasing with the dMn concentrations suggesting a hydrothermal origin of the Cu-ligands detected. For the first time, the apparent L concentrations were discussed in line with the *in situ* concentrations of free inorganic sulfides. In the early mixing, it appeared that L concentrations were following the trend of ΣS when plotting both parameters against dMn. The corresponding stability constants of Cu-ligands (log K'_{CuL} ; avg. 12.9) were similar to those already reported for strong organic ligands (e.g. thiols, log K'_{CuL} ~ 13) in deep sea hydrothermal vents [10] but also to that of inorganic sulfide complexes (log K'_{CuHS}) [50]. Taking into account the experimental conditions used in the present work, the apparent copper binding capacity measured in all samples was likely a combination of strong organosulfur complexes and stable inorganic Cu-sulfide complexes, able to resist to the progressive oxidization of samples. However, the inorganic sulfides, present at massive concentrations *in situ*, are probably the major ligand involved in the stabilization of hydrothermally sourced copper in this area, as suggested in earlier work [8,9]. Based on the work of Al-Farawati and van den Berg [50] and on sulfides concentrations greater than 100 µM in most of our samples, we inferred that Cu bindings ligands could be predominantly inorganic

sulfur species in the early mixing. This does not invalidate the previous finding on organic copper complexation in hydrothermal vents. The assumption made here is rather that the impact of the organosulfur ligands on Cu-stabilization should be much lower than the one of inorganic sulfides in the buoyant plume because of their low concentration in comparison to sulfides. However, with the aging of the plume, the progressive oxidization of free sulfides and some local mixing with biologically rich diffuse vents, the part of organic ligand should increase, as well as its role on Cu-stabilization. Organosulfur compounds and stabilized sulfides might therefore coexist in the buoyant and neutrally buoyant plume, until the complete oxidation of inorganic sulfides complexes. Finally, our results indicate that this mixture partly resists to strong oxidizing conditions (air-purging) suggesting that copper could be transported far from the vent sources.

Acknowlegdements

We wish to thank the captains and crew of the two R/V Pourquoi Pas? and Atalante. We are grateful to the Victor 6000 ROV pilots for their assistance at sea, Mathilde Cannat and Jérôme Blandin coordinators of the projects and cruises, Nicolas Gayet for his help in collecting the samples, Céline Liorzou and Marie-Laure Rouget (PSO) for the ICP-AES and ICP-MS measurements. We would like to thank Irena Ciglenečki-Jušić and Zdeslav Zovko for DOC measurements. This work was funded by grants from Ifremer and Université de Bretagne Occidentale (DEI). We acknowledge financial support from the French ANR Luckyscales project (ANR-14-CE02-0008-02) and the EU project EMSO (http://www.emso-eu.org/) (PhD grant to L. Cotte). This work was also supported by the MEBTRACE project granted by the Croatian Science Foundation (IP–2014–09–7530; PI: DO). Finally, we are grateful to two

705 anonymous reviewers and the editor Peter Croot for their helpful and constructive comments.
706 The authors declare no conflicts of interest.
707

References

[1] K. Hirose, Chemical speciation of trace metals in seawater: a review, *Analytical Sciences* **2006**, *22*, 1055–1063.

[2] J.C. Alt, Subseafloor processes in Mid-Ocean Ridge hydrothermal systems, *Seafloor Hydrothermal Systems: Physical, Chemical, Biological, and Geological Interactions, Geophysical Monograph Series* **1995**, *91*, 85–114.

[3] J.L. Charlou, J.P. Donval, E. Douville, P. Jean-Baptiste, J. Radford-Knoery, Y. Fouquet, A. Dapoigny, M. Stievenard, Compared geochemical signatures and the evolution of Menez Gwen (37°50′N) and Lucky Strike (37°17′N) hydrothermal fluids, south of the Azores Triple Junction on the Mid-Atlantic Ridge, *Chemical Geology* **2000**, *171*, 49–75. doi:10.1016/S0009-2541(00)00244-8.

[4] E.P. Reeves, J.M. McDermott, J.S. Seewald, The origin of methanethiol in midocean ridge hydrothermal fluids, *Proceedings of the National Academy of Sciences* **2014**, *111*, 5474–5479.

[5] T.M. McCollom, J.S. Seewald, C.R. German, Investigation of extractable organic compounds in deep-sea hydrothermal vent fluids along the Mid-Atlantic Ridge, *Geochimica et Cosmochimica Acta* **2015**, *156*, 122–144. doi:10.1016/j.gca.2015.02.022.

[6] V. Klevenz, W. Bach, K. Schmidt, M. Hentscher, A. Koschinsky, S. Petersen, Geochemistry of vent fluid particles formed during initial hydrothermal fluid–seawater mixing along the Mid-Atlantic Ridge, *Geochemistry, Geophysics, Geosystems* **2011**, *12*, 1–23. doi:10.1029/2011GC003704.

[7] J.M. Edmond, C. Measures, R.E. McDuff, L.H. Chan, R. Collier, B. Grant, L.I. Gordon, J.B. Corliss, Ridge crest hydrothermal activity and the balances of the major and minor elements in the ocean: The Galapagos data, *Earth and Planetary Science Letters* **1979**, *46*, 1–18. doi:10.1016/0012-821X(79)90061-X.

[8] G.W. Luther, T.F. Rozan, M. Taillefert, D.B. Nuzzio, C. Di Meo, T.M. Shank, R.A. Lutz, S.C. Cary, Chemical speciation drives hydrothermal vent ecology, *Nature* **2001**, *410*, 813–816. doi:10.1038/35071069.

[9] V.P. Edgcomb, S.J. Molyneaux, M.A. Saito, K. Lloyd, S. Böer, C.O. Wirsen, M.S. Atkins, A. Teske, Sulfide ameliorates metal toxicity for deep-sea hydrothermal vent archaea, *Applied and Environmental Microbiology* **2004**, *70*, 2551–2555.

[10] S.G. Sander, A. Koschinsky, G. Massoth, M. Stott, K.A. Hunter, Organic complexation of copper in deep-sea hydrothermal vent systems, *Environmental Chemistry* **2007**, *4*, 81–89.

[11] Z.D. Powell, Voltammetric studies on the stabilisation of dissolved copper in hydrothermal vent fluids, *PhD Thesis, University of Otago, Dunedin, New Zealand* **2014**.

[12] C. Kleint, S. Kuzmanovski, Z. Powell, S.I. Bühring, S.G. Sander, A. Koschinsky, Organic Cu-complexation at the shallow marine hydrothermal vent fields off the coast of Milos (Greece), Dominica (Lesser Antilles) and the Bay of Plenty (New Zealand), *Marine Chemistry* **2015**, *173*, 244–252. doi:10.1016/j.marchem.2014.10.012.

[13] S.G. Sander, A. Koschinsky, Metal flux from hydrothermal vents increased by organic complexation, *Nature Geoscience* **2011**, *4*, 145–150. doi:10.1038/ngeo1088.

[14] S.A. Bennett, E.P. Achterberg, D.P. Connelly, P.J. Statham, G.R. Fones, C.R. German, The distribution and stabilisation of dissolved Fe in deep-sea hydrothermal plumes, *Earth and Planetary Science Letters* **2008**, *270*, 157–167. doi:10.1016/j.epsl.2008.01.048.

[15] J.A. Hawkes, D.P. Connelly, M. Gledhill, E.P. Achterberg, The stabilisation and transportation of dissolved iron from high temperature hydrothermal vent systems, *Earth and Planetary Science Letters* **2013**, *375*, 280–290. doi:10.1016/j.epsl.2013.05.047.
[16] C. Kleint, J.A. Hawkes, S.G. Sander, A. Koschinsky, Voltammetric investigation of hydrothermal iron speciation, *Frontiers in Marine Science* **2016**, *3*, 75. doi:10.3389/fmars.2016.00075.
[17] H. Whitby, C.M.G. van den Berg, Evidence for copper-binding humic substances in seawater, *Marine Chemistry* **2015**, *173*, 282–290. doi:10.1016/j.marchem.2014.09.011.
[18] C.R. DeMets, R.G. Gordon, D.F. Argus, S. Stein, Current plate motions, *Geophysical Journal International* **1990**, *101*, 425–478.
[19] M. Cannat, A. Briais, C. Deplus, J. Escartín, J. Georgen, J. Lin, S. Mercouriev, C. Meyzen, M. Muller, G. Pouliquen, A. Rabain, P. da Silva, Mid-Atlantic Ridge–Azores hotspot interactions: along-axis migration of a hotspot-derived event of enhanced magmatism 10 to 4 Ma ago, *Earth and Planetary Science Letters* **1999**, *173*, 257–269.
[20] S.E. Humphris, D.J. Fornari, D.S. Scheirer, C.R. German, L.M. Parson, Geotectonic setting of hydrothermal activity on the summit of Lucky Strike Seamount (37°17′N, Mid-Atlantic Ridge), *Geochemistry, Geophysics, Geosystems* **2002**, *3*, 1–24.
[21] Y. Fouquet, H. Ondréas, J.L. Charlou, J.P. Donval, J. Radford-Knoery, I. Costa, N. Lourenco, M.K. Tivey, Atlantic lava lakes and hot vents, *Nature* **1995**, *377*, 201–201. doi:10.1038/377201a0.
[22] H. Ondréas, M. Cannat, Y. Fouquet, A. Normand, P.M. Sarradin, J. Sarrazin, Recent volcanic events and the distribution of hydrothermal venting at the Lucky Strike hydrothermal field, Mid-Atlantic Ridge, *Geochemistry, Geophysics, Geosystems* **2009**, *10*, 1–18. doi:10.1029/2008GC002171.
[23] T. Barreyre, J. Escartín, R. Garcia, M. Cannat, E. Mittelstaedt, R. Prados, Structure, temporal evolution, and heat flux estimates from the Lucky Strike deep-sea hydrothermal field derived from seafloor image mosaics, *Geochemistry, Geophysics, Geosystems* **2012**, *13*, 1–29. doi:10.1029/2011GC003990.
[24] P.M. Sarradin, Sarrazin, J., Allais, A. G., Almeida, D., B. V., Boetius, A., Buffier, E., Coiras, E., Colaco, A., Cormack, A., Dentrecolas, S., Desbruyeres, D., Dorval, P., du Buf, H., Dupont, J., Godfroy, A., Gouillou, M., Gronemann, J., Hamel, G., Hamon, M., Hoge, U., Lane, D., Le Gall, C., Leroux, D., Legrand, J., Leon, P., Leveque, J. P., Masson, M., Olu, K., Pascoal, A., Sauter, E., Sanfilippo, L., Savino, E., Sebastiao, L., Santos, R. S., Shillito, B., Simeoni, P., Schultz, A., Sudreau, J. P., Taylor, P., Vuillemin, R., Waldmann, C., Wenzhöfer, F., Zal, F., EXtreme ecosystem studies in the deep OCEan: Technological developments, *Ieee* **2007**, *1–3*.
[25] R. Vuillemin, D. Le Roux, P. Dorval, K. Bucas, J.P. Sudreau, M. Hamon, C. Le Gall, P.M. Sarradin, CHEMINI: A new in situ CHEmical MINIaturized analyzer, *Deep Sea Research I* **2009**, *56*, 1391–1399. doi:10.1016/j.dsr.2009.02.002.
[26] N. Le Bris, P.M. Sarradin, D. Birot, A.M. Alayse-Danet, A new chemical analyzer for in situ measurement of nitrate and total sulfide over hydrothermal vent biological communities, *Marine Chemistry* **2000**, *72*, 1–15. doi:10.1016/S0304-4203(00)00057-8.
[27] K.N. Buck, J. Moffett, K.A. Barbeau, R.M. Bundy, Y. Kondo, J. Wu, The organic complexation of iron and copper: An intercomparison of competitive ligand exchange-adsorptive cathodic stripping voltammetry (CLE-ACSV) techniques, *Limnology and Oceanography: Methods* **2012**, *10*, 496–515. doi:10.4319/lom.2012.10.496.
[28] M.L.A.M. Campos, C.M.G. van den Berg, Determination of copper complexation in sea water by cathodic stripping voltammetry and ligand competition with salicylaldoxime, *Analytica Chimica Acta* **1994**, *284*, 481–496. doi:10.1016/0003-2670(94)85055-0.

[29] C. Garnier, I. Pižeta, S. Mounier, J.Y. Benaïm, M. Branica, Influence of the type of titration and of data treatment methods on metal complexing parameters determination of single and multi-ligand systems measured by stripping voltammetry, *Analytica Chimica Acta* **2004**, *505*, 263–275. doi:10.1016/j.aca.2003.10.066.
[30] D. Omanović, C. Garnier, I. Pižeta, ProMCC: An all-in-one tool for trace metal complexation studies, *Marine Chemistry* **2015**, *173*, 25–39. doi:10.1016/j.marchem.2014.10.011.
[31] I. Pižeta, S.G. Sander, R.J.M. Hudson, D. Omanović, O. Baars, K.A. Barbeau, K.N. Buck, R.M. Bundy, G. Carrasco, P.L. Croot, C. Garnier, L.J.A. Gerringa, M. Gledhill, K. Hirose, Y. Kondo, L.M. Laglera, J. Nuester, M.J.A. Rijkenberg, S. Takeda, B.S. Twining, M. Wells, Interpretation of complexometric titration data: An intercomparison of methods for estimating models of trace metal complexation by natural organic ligands, *Marine Chemistry* **2015**, *173*, 3–24. doi:10.1016/j.marchem.2015.03.006.
[32] D. Omanović, M. Branica, Automation of voltammetric measurements by polarographic analyser PAR 384B., *Croatica Chemica Acta* **1998**, *71*, 421–433.
[33] I. Pižeta, D. Omanović, M. Branica, The influence of data treatment on the interpretation of experimental results in voltammetry, *Analytica Chimica Acta* **1999**, *401*, 163–172. doi:10.1016/S0003-2670(99)00491-2.
[34] D. Omanović, C. Garnier, Y. Louis, V. Lenoble, S. Mounier, I. Pižeta, Significance of data treatment and experimental setup on the determination of copper complexing parameters by anodic stripping voltammetry, *Analytica Chimica Acta* **2010**, *664*, 136–143. doi:10.1016/j.aca.2010.02.008.
[35] I. Ciglenečki, D. Krznarić, G.R. Helz, Voltammetry of copper sulfide particles and nanoparticles: Investigation of the cluster hypothesis, *Environmental Science & Technology* **2005**, *39*, 7492–7498. doi:10.1021/es050586v.
[36] D. Krznarić, G.R. Helz, I. Ciglenečki, Prospect of determining copper sulfide nanoparticles by voltammetry: A potential artifact in supersaturated solutions, *Journal of Electroanalytical Chemistry* **2006**, *590*, 207–214. doi:10.1016/j.jelechem.2006.03.046.
[37] D. Krznarić, G.R. Helz, E. Bura-Nakić, D. Jurašin, Accumulation mechanism for metal chalcogenide nanoparticles at Hg^0 electrodes: Copper sulfide example, *Analytical Chemistry* **2008**, *80*, 742–749. doi:10.1021/ac071180z.
[38] D. Omanović, Z. Kwokal, A. Goodwin, A. Lawrence, C.E. Banks, R.G. Compton, S. Komorsky-Lovrić, Trace metal detection in Sibenik Bay, Croatia: Cadmium, lead and copper with anodic stripping voltammetry and manganese via sonoelectrochemistry. A case study, *Journal of the Iranian Chemical Society* **2006**, *3*, 128–139. doi:10.1007/BF03245940.
[39] Y. Louis, P. Cmuk, D. Omanović, C. Garnier, V. Lenoble, S. Mounier, I. Pižeta, Speciation of trace metals in natural waters: The influence of an adsorbed layer of natural organic matter (NOM) on voltammetric behaviour of copper, *Analytica Chimica Acta* **2008**, *606*, 37–44. doi:10.1016/j.aca.2007.11.011.
[40] L. Cotte, M. Waeles, B. Pernet-Coudrier, P.M. Sarradin, C. Cathalot, R.D. Riso, A comparison of in situ vs. ex situ filtration methods on the assessment of dissolved and particulate metals at hydrothermal vents, *Deep Sea Research I* **2015**, *105*, 186–194. doi:http://dx.doi.org/10.1016/j.dsr.2015.09.005.
[41] S.L. Simpson, S.C. Apte, G.E. Batley, Sample storage artifacts affecting the measurement of dissolved copper in sulfidic waters, *Analytical Chemistry* **1998**, *70*, 4202–4205. doi:10.1021/ac980006v.
[42] R. Benner, M. Strom, A critical evaluation of the analytical blank associated with DOC measurements by high-temperature catalytic oxidation, *Marine Chemistry* **1993**, *41*, 153–160. doi:10.1016/0304-4203(93)90113-3.

853 [43] J.P. Cowen, G.J. Massoth, R.A. Feely, Scavenging rates of dissolved manganese in a
854 hydrothermal vent plume, *Deep Sea Research A* **1990**, *37*, 1619–1637. doi:10.1016/0198-
855 0149(90)90065-4.
856 [44] M.P. Field, R.M. Sherrell, Dissolved and particulate Fe in a hydrothermal plume at
857 9°45′N, East Pacific Rise: Slow Fe (II) oxidation kinetics in Pacific plumes, *Geochimica*
858 *et Cosmochimica Acta* **2000**, *64*, 619–628. doi:10.1016/S0016-7037(99)00333-6.
859 [45] P.A. Yeats, J.A. Dalziel, S.B. Moran, A comparison of dissolved and particulate Mn and
860 Al distributions in the Western North-Atlantic, *Oceanologica Acta* **1992**, *15*, 609–619.
861 [46] P.J.M. Buckley, C.M.G. van den Berg, Copper complexation profiles in the Atlantic
862 Ocean: A comparative study using electrochemical and ion exchange techniques, *Marine*
863 *Chemistry* **1986**, *19*, 281–296. doi:10.1016/0304-4203(86)90028-9.
864 [47] J.E. Jacquot, J.W. Moffett, Copper distribution and speciation across the International
865 GEOTRACES Section GA03, *Deep Sea Research II* **2015**, *116*, 187–207.
866 doi:10.1016/j.dsr2.2014.11.013.
867 [48] M. Waeles, L. Cotte, B. Pernet-Coudrier, V. Chavagnac, C. Cathalot, T. Leleu, A. Laës-
868 Huon, A. Perhirin, R.D. Riso, P.-M. Sarradin, On the early fate of hydrothermal iron at
869 deep-sea vents: A reassessment after in-situ filtration, *Geophysical Research Letters* **2017**,
870 1–8. doi:10.1002/2017GL073315.
871 [49] I. Ciglenečki, B. Ćosović, Electrochemical study of sulfur species in seawater and marine
872 phytoplankton cultures, *Marine Chemistry* **1996**, *52*, 87–97. doi:10.1016/0304-
873 4203(95)00080-1.
874 [50] R. Al-Farawati, C.M.G. van den Berg, Metal–sulfide complexation in seawater, *Marine*
875 *Chemistry* **1999**, *63*, 331–352. doi:10.1016/S0304-4203(98)00056-5.
876 [51] I. Ciglenečki, B. Ćosović, Electrochemical determination of thiosulfate in seawater in the
877 presence of elemental sulfur and sulfide, *Electroanalysis* **1997**, *9*, 775–780.
878 doi:10.1002/elan.1140091009.
879 [52] F. Wang, A. Tessier, J. Buffle, Voltammetric determination of elemental sulfur in pore
880 waters, *Limnology and Oceanography* **1998**, *43*, 1353–1361.
881 [53] I. Ciglenečki, E. Bura-Nakić, M. Marguš, Zinc sulfide surface formation on Hg electrode
882 during cyclic voltammetric scan: an implication for previous and future research studies
883 on metal sulfide systems, *Journal of Solid State Electrochemistry* **2012**, *16*, 2041–2046.
884 doi:10.1007/s10008-011-1612-4.
885 [54] I. Ciglenečki, M. Marguš, E. Bura-Nakić, I. Milanović, Electroanalytical methods in
886 characterization of sulfur species in aqueous environment, *Journal of Electrochemical*
887 *Science and Engineering* **2014**, *4*, 155–163.
888 [55] I. Milanović, D. Krznarić, E. Bura-Nakić, I. Ciglenečki, Deposition and dissolution of
889 metal sulfide layers at the Hg electrode surface in seawater electrolyte conditions,
890 *Environmental Chemistry* **2013**, *11*, 167–172.
891 [56] T.F. Rozan, S.M. Theberge, G. Luther, Quantifying elemental sulfur (S^0), bisulfide (HS^-)
892 and polysulfides (S_x^{2-}) using a voltammetric method, *Analytica Chimica Acta* **2000**, *415*,
893 175–184. doi:10.1016/S0003-2670(00)00844-8.
894 [57] E. Bura-Nakić, D. Krznarić, D. Jurašin, G.R. Helz, I. Ciglenečki, Voltammetric
895 characterization of metal sulfide particles and nanoparticles in model solutions and natural
896 waters, *Analytica Chimica Acta* **2007**, *594*, 44–51. doi:10.1016/j.aca.2007.04.065.
897 [58] E. Bura-Nakić, D. Krznarić, G.R. Helz, I. Ciglenečki, Characterization of iron sulfide
898 species in model solutions by cyclic voltammetry. Revisiting an old problem,
899 *Electroanalysis* **2011**, *23*, 1376–1382. doi:10.1002/elan.201000675.
900 [59] R. Al-Farawati, C.M.G. van den Berg, The determination of sulfide in seawater by flow-
901 analysis with voltammetric detection, *Marine Chemistry* **1997**, *57*, 277–286.
902 doi:10.1016/S0304-4203(97)00014-5.

[60] L.M. Laglera, C.M.G. van den Berg, Copper complexation by thiol compounds in estuarine waters, *Marine Chemistry* **2003**, *82*, 71–89. doi:10.1016/S0304-4203(03)00053-7.
[61] A. Gartman, M. Yücel, A.S. Madison, D.W. Chu, S. Ma, C.P. Janzen, E.L. Becker, R.A. Beinart, P.R. Girguis, G.W. Luther, Sulfide oxidation across diffuse flow zones of hydrothermal vents, *Aquatic Geochemistry* **2011**, *17*, 583–601. doi:10.1007/s10498-011-9136-1.
[62] V. Klevenz, S.G. Sander, M. Perner, A. Koschinsky, Amelioration of free copper by hydrothermal vent microbes as a response to high copper concentrations, *Chemistry and Ecology* **2012**, *28*, 405–420. doi:10.1080/02757540.2012.666531.
[63] A.G. González, N. Pérez-Almeida, J. Magdalena Santana-Casiano, F.J. Millero, M. González-Dávila, Redox interactions of Fe and Cu in seawater, *Marine Chemistry* **2016**, *179*, 12–22. doi:10.1016/j.marchem.2016.01.004.
[64] M.F.C. Leal, C.M.G. van den Berg, Evidence for strong copper(I) complexation by organic ligands in seawater, *Aquatic Geochemistry* **1998**, *4*, 49–75. doi:10.1023/A:1009653002399.
[65] M.J. Walsh, B.A. Ahner, Determination of stability constants of Cu(I), Cd(II) & Zn(II) complexes with thiols using fluorescent probes, *Journal of Inorganic Biochemistry* **2013**, *128*, 112–123. doi:10.1016/j.jinorgbio.2013.07.012.
[66] N. Pérez-Almeida, M. González-Dávila, J. Magdalena Santana-Casiano, A.G. González, M. Suárez de Tangil, Oxidation of Cu(I) in seawater at low oxygen concentrations, *Environmental Science & Technology* **2013**, *47*, 1239–1247. doi:10.1021/es302465d.
[67] D.A. Hansell, Recalcitrant dissolved organic carbon fractions, *Annual Review of Marine Science* **2013**, *5*, 421–445.
[68] L. Guo, P.H. Santschi, K.W. Warnken, Dynamics of dissolved organic carbon (DOC) in oceanic environments, *Limnology and Oceanography* **1995**, *40*, 1392–1403. doi:10.4319/lo.1995.40.8.1392.
[69] D.A. Hansell, C.A. Carlson, Deep-ocean gradients in the concentration of dissolved organic carbon, *Nature* **1998**, *395*, 263–266. doi:10.1038/26200.
[70] S.Q. Lang, D.A. Butterfield, M.D. Lilley, H. Paul Johnson, J.I. Hedges, Dissolved organic carbon in ridge-axis and ridge-flank hydrothermal systems, *Geochimica et Cosmochimica Acta* **2006**, *70*, 3830–3842. doi:10.1016/j.gca.2006.04.031.
[71] J.A. Hawkes, P.E. Rossel, A. Stubbins, D. Butterfield, D.P. Connelly, E.P. Achterberg, A. Koschinsky, V. Chavagnac, C.T. Hansen, W. Bach, T. Dittmar, Efficient removal of recalcitrant deep-ocean dissolved organic matter during hydrothermal circulation, *Nature Geoscience* **2015**, *8*, 856–860.
[72] S.A. Bennett, P.J. Statham, D.R.H. Green, N. Le Bris, J.M. McDermott, F. Prado, O.J. Rouxel, K. Von Damm, C.R. German, Dissolved and particulate organic carbon in hydrothermal plumes from the East Pacific Rise, 9°50′N, *Deep Sea Research I* **2011**, *58*, 922–931. doi:10.1016/j.dsr.2011.06.010.
[73] J.A. Hawkes, C.T. Hansen, T. Goldhammer, W. Bach, T. Dittmar, Molecular alteration of marine dissolved organic matter under experimental hydrothermal conditions, *Geochimica et Cosmochimica Acta* **2016**, *175*, 68–85. doi:10.1016/j.gca.2015.11.025.
[74] C. Konn, J.L. Charlou, N.G. Holm, O. Mousis, The production of methane, hydrogen, and organic compounds in ultramafic-hosted hydrothermal vents of the Mid-Atlantic Ridge, *Astrobiology* **2015**, *15*, 381–399.
[75] M.D. Schulte, K.L. Rogers, Thiols in hydrothermal solution: standard partial molal properties and their role in the organic geochemistry of hydrothermal environments, *Geochimica et Cosmochimica Acta* **2004**, *68*, 1087–1097. doi:10.1016/j.gca.2003.06.001.

[76] J.L. Charlou, J.P. Donval, C. Konn, H. Ondréas, Y. Fouquet, P. Jean-Baptiste, E. Fourré, High production and fluxes of H_2 and CH_4 and evidence of abiotic hydrocarbon synthesis by serpentinization in ultramafic-hosted hydrothermal systems on the Mid-Atlantic Ridge, *Diversity of Hydrothermal Systems on Slow Spreading Ocean Ridges, Geophysical Monograph Series* **2010**, *188*, 265–296.
[77] M. Bailly-Bechet, M. Kerszberg, F. Gaill, F. Pradillon, A modeling approach of the influence of local hydrodynamic conditions on larval dispersal at hydrothermal vents, *Journal of Theoretical Biology* **2008**, *255*, 320–331. doi:10.1016/j.jtbi.2008.08.016.
[78] M.C. Lohan, D.W. Crawford, D.A. Purdie, P.J. Statham, Iron and zinc enrichments in the northeastern subarctic Pacific: Ligand production and zinc availability in response to phytoplankton growth, *Limnology and Oceanography* **2005**, *50*, 1427–1437.
[79] B.W. Mountain, T.M. Seward, Hydrosulfide/sulfide complexes of copper(I): Experimental confirmation of the stoechiometry and stability of $Cu(HS)_2^-$ to elevated temperatures, *Geochimica et Cosmochimica Acta* **2003**, *67*, 3005–3014. doi:10.1016/S0016-7037(03)00303-X.
[80] J.Z. Zhang, F.J. Millero, Investigation of metal sulfide complexes in sea water using cathodic stripping square wave voltammetry, *Analytica Chimica Acta* **1994**, *284*, 497–504. doi:10.1016/0003-2670(94)85056-9.
[81] E. Mittelstaedt, J. Escartín, N. Gracias, J.A. Olive, T. Barreyre, A. Davaille, M. Cannat, R. Garcia, Quantifying diffuse and discrete venting at the Tour Eiffel vent site, Lucky Strike hydrothermal field, *Geochemistry, Geophysics, Geosystems* **2012**, *13*, 1–18. doi:10.1029/2011GC003991.
[82] T.F. Rozan, G. Benoit, G.W. Luther, Measuring metal sulfide complexes in oxic river waters with square wave voltammetry, *Environmental Science & Technology* **1999**, *33*, 3021–3026. doi:10.1021/es981206r.
[83] P.J. Superville, I. Pižeta, D. Omanović, G. Billon, Identification and on-line monitoring of reduced sulphur species (RSS) by voltammetry in oxic waters, *Talanta* **2013**, *112*, 55–62.

983 **Table 1.** Calculated complexing parameters for Cu (L and K'_{CuL}) obtained in untreated samples (2015)
984 from Aisics and Y3 hydrothermal vents (Lucky Strike, MAR). Mean temperature (recorded during
985 sampling) as well as natural pH, total dissolved manganese (dMn) and total dissolved copper (dCu)
986 concentrations measured are also provided.

Site	Sample	T_{PEPITO}	pH	dMn	dCu	L	$logK'_{CuL}$
		°C		µM	nM	nM	
Aisics	02598 A1	5.27	7.5	1.08	12	-	-
	02598 A3	17.2	6.1	11.1	129	-	-
	02598 B1	31.1	5.6	19.9	771	2104 ± 126	12.86 ± 0.15
	02598 B3	47.0	5.1	23.6	32	230 ± 12	13.03 ± 0.07
	02598 C1	57.0	5.3	37.2	39	377 ± 15	12.68 ± 0.05
	02598 C2	72.6	5.2	48.8	212	746 ± 30	13.38 ± 0.07
	02598 C3	67.6	5.2	44.9	119	1059 ± 74	12.95 ± 0.10
	02598 D1	55.0	5.3	39.4	26	351 ± 23	12.95 ± 0.08
	02598 D2	96.7	5.0	64.3	63	768 ± 88	12.91 ± 0.17
	02598 D3	108	4.9	72.9	456	2972 ± 156	12.97 ± 0.08
	02598 E1	121	4.9	83.4	50	336 ± 25	12.37 ± 0.07
	02598 E3	154	4.7	102	312	742 ± 89	12.99 ± 0.20
Y3	10606 A1	4.97	7.4	0.65	13	32.5 ± 2.6	12.55 ± 0.09
	10606 A2	10.0	6.7	4.26	32	61.5 ± 5.5	12.96 ± 0.14
	10606 A3	20.3	6.2	11.8	76	175 ± 12	12.89 ± 0.08
	10606 B2	35.4	5.8	26.9	365	519 ± 20	13.15 ± 0.09
	10606 B3	50.3	5.6	36.2	234	294 ± 46	12.69 ± 0.32
	10606 C1	60.1	5.5	44.4	102	499 ± 25	12.57 ± 0.05
	10606 C2	68.8	5.5	47.9	409	740 ± 37	12.95 ± 0.10
	10606 C3	80.4	5.4	70.8	325	585 ± 35	12.98 ± 0.10
	10606 D1	88.8	5.3	65.2	335	1024 ± 33	13.13 ± 0.05

987

988 **Table 2.** Calculated complexing parameters for Cu (L^* and K'^*_{CuL}) and dissolved Cu concentrations
989 (dCu^*) obtained in pretreated (air purged-filtered) samples from Aisics hydrothermal vent (2016). Mean
990 temperature (recorded during sampling) as well as natural pH, total dissolved manganese (dMn), total
991 dissolved copper (dCu) and DOC concentrations obtained before any pretreatment of these samples are
992 also provided.

Site	Sample	T_{PEPITO}	pH	dMn	dCu	dCu^*	DOC	L^*	$logK'^*_{CuL}$
		°C		µM	nM	nM	µM	nM	
Aisics	09632 A1	5.40	7.5	1.90	-	2.5	55.5	-	-
	09632 A2	12.7	5.8	5.03	7	3.6	55.6	-	-
	09632 A3	19.1	5.4	9.85	121	3.5	49.3	-	-
	09632 B1	32.2	5.1	14.0	277	10	59.1	22.8 ± 1.2	13.04 ± 0.05
	09632 B2	56.4	5.4	42.5	55	14	51.2	26.9 ± 7.5	12.75 ± 0.32
	09632 B3	73.6	5.2	38.4	410	-	-	-	-
	09632 C1	87.5	4.6	68.8	-	6.2	24.8	18.2 ± 1.0	12.61 ± 0.05
	09632 C2	114	4.7	77.5	-	6.3	40.8	41.8 ± 2.9	12.57 ± 0.06
	09632 C3	126	4.6	70.9	42	3.1	89.8	43.9 ± 5.1	12.96 ± 0.10

993

994 **Table 3.** Concentrations of ΣS (H_2S, HS^-, S^{2-}) and O_2 obtained with *in situ* instruments at Aisics and
995 Y3 hydrothermal vents. In order to plot all *in situ* parameters as a function of dMn, the corresponding
996 manganese concentrations ($dMn_{\Sigma S}$) were estimated from $T_{CHEMINI}$ thanks to the linear dMn-T_{PEPITO}
997 relationship obtained at Aisics and Y3 (see SI).

Site and date	Sample	$T_{CHEMINI(\Sigma S)}$	$dMn_{\Sigma S}$	ΣS	O_2
		°C	µM	µM	µM
Aisics (02598-2015)	02598 A1	5.18	0.83	0.98	276
	02598 A3	17.2	11.1	27.7	230
	02598 B1	31.1	19.9	62.6	243
	02598 B3	47.0	23.6	138	210
	02598 C1	57.0	37.2	321	190
	02598 C2	72.6	48.8	265	215
	02598 C3	67.6	44.9	237	189
	02598 D1	55.0	39.4	250	219
	02598 D2	96.7	64.3	231	186
	02598 D3	108	72.9	191	143
	02598 E1	121	83.4	169	162
	02598 E3	154	102	187	146
Aisics (09632-2016)	09632 A1	7.98	2.71	5.25	-
	09632 A2	11.4	5.03	89.0	-
	09632 A3	19.5	10.6	160	-
	09632 B1	30.3	17.9	224	-
	09632 B2	54.1	34.1	263	-
	09632 B3	60.0	38.1	286	-
	09632 C1	108	70.7	320	-
	09632 C2	117	76.6	335	-
	09632 C3	120	78.9	352	-
Y3 (07582-2014)	07582 A1	5.98	1.47	77.7	-
	07582 A2	9.90	4.37	52.2	-
	07582 A3	23.4	14.4	132	-
	07582 B1	45.1	30.4	275	-
	07582 B2	54.7	37.5	286	-
	07582 B3	78.2	55.0	363	-
	07582 C1	97.5	69.3	415	-
	07582 C2	70.8	49.5	266	-
Y3 (10606-2015)	10606 A1	-	-	-	247
	10606 A2	-	-	-	-
	10606 A3	-	-	-	264
	10606 B2	-	-	-	249
	10606 B3	-	-	-	240
	10606 C1	-	-	-	209
	10606 C2	-	-	-	242
	10606 C3	-	-	-	183
	10606 D1	-	-	-	183

998

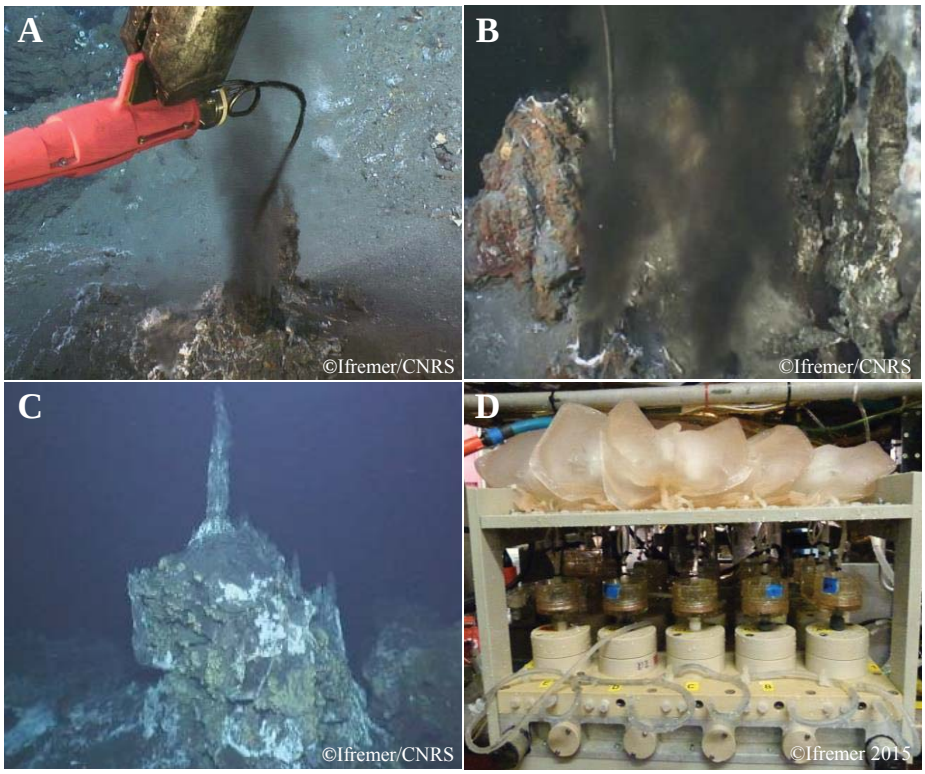

Figure 1. (A) Main black smoker Aisics (Endmember temperature: 307°C) at the Lucky strike vent field (MAR) sampled during the Momarsat 2015 and 2016 cruises using the PEPITO sampler. The titanium-Silicon inlet coupled to the ROV temperature probe is also shown. **(B)** Main black smoker Y3 (Endmember temperature: 326°C) during sampling. **(C)** Overall view of the site Y3, Lucky Strike (MAR). **(D)** PEPITO sampler implemented on the ROV with freshly collected samples filtered *in-situ*. The reader might see that 2 PVC-bags were attached to each filter holder: 2 bags for each sample were thus collected in 2015. After recovery, one bag was frozen at -20°C whereas the other one was poisoned with NaN_3 and stored at 4°C with the aim to compare the impact of sample storage on Cu speciation. As freezing was suspected to worsen the aggregation of colloidal phases, only poisoned bags were analyzed at that moment. Samples collected in 2016 were treated the same way, as indicated in the text.

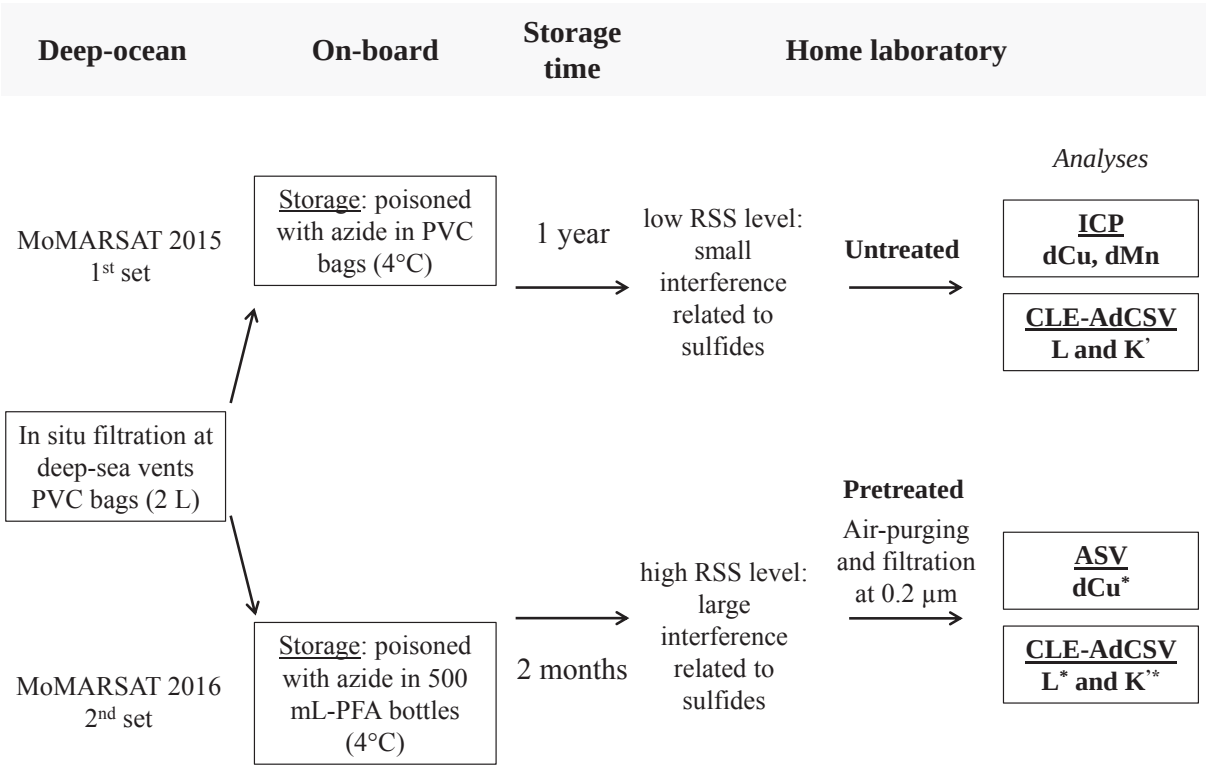

Figure 2. Summary diagram of the strategy used from the storage to the analyses for the assessment of the Cu complexing parameters. Samples stored in PFA-bottles were also analyzed by ICP for total dissolved copper (dCu) before being pretreated (see paragraph 2.5). RSS denote Reduced sulfide species.

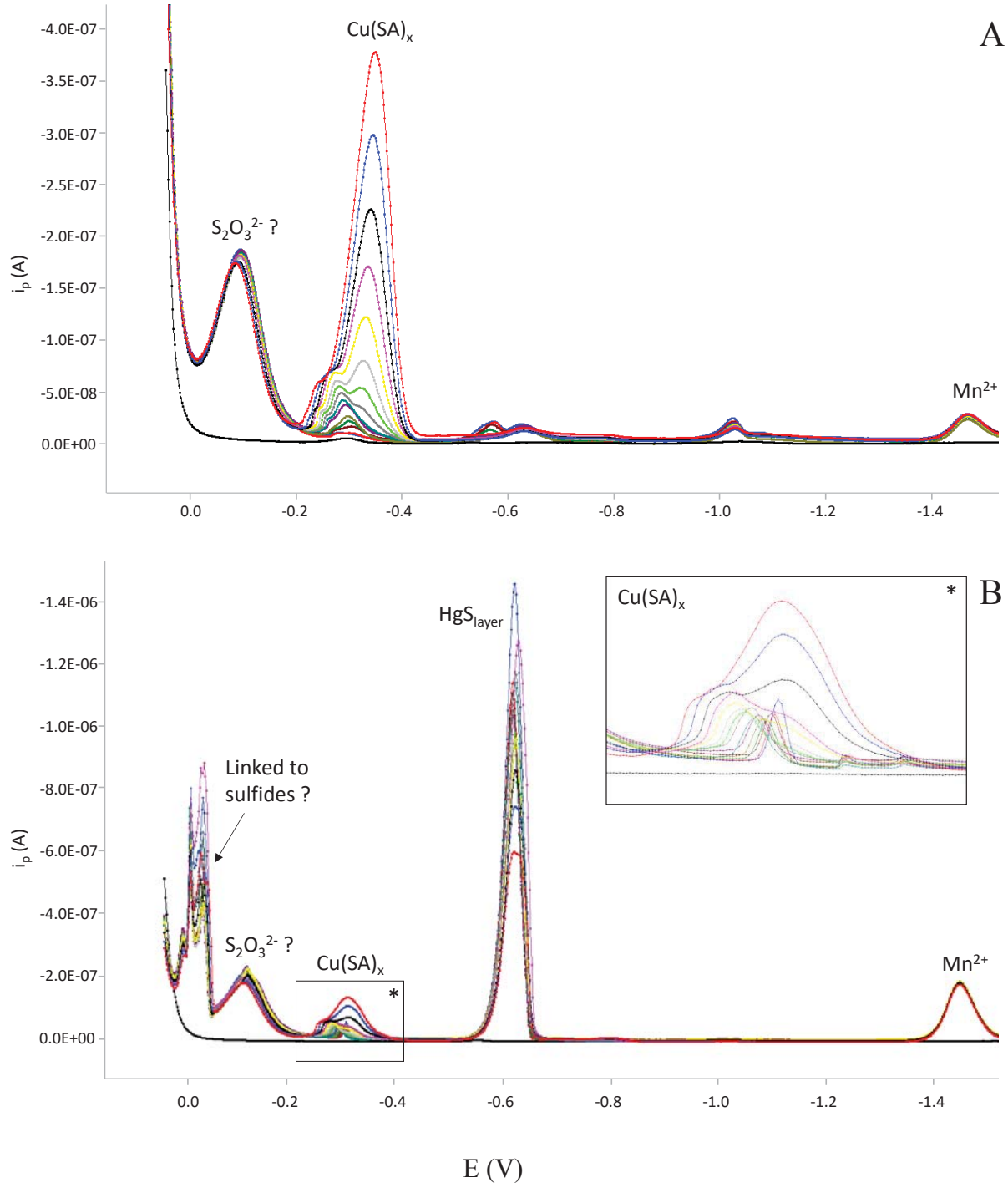

Figure 3. A) Typical voltammogram obtained for complexometric titrations in the untreated samples (1st set; e.g. 02598 C1). Untreated samples were 10-fold diluted in UVSW. B) Typical voltammogram obtained for the pretreated samples (e.g. 09632 C3). The right panel shows all $Cu(SA)_x$ signals for the whole titration experiment. The detailed scale of potential in the inset is provided in Figure S3. All titration experiments were performed after overnight equilibration at pH ~ 8.2 and 4 µM SA. Black signals correspond to the blank (UVSW). The $Cu(SA)_x$ signal was extracted from the interfering signals (i.e. 'shoulders' at -0.27 V vs Ag/AgCl) observed at low additions of Cu for both sets of samples.

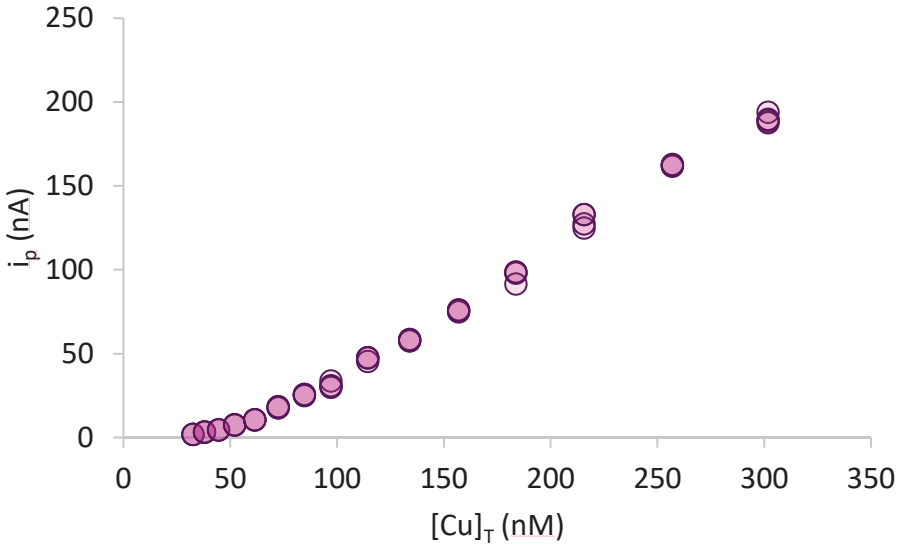

Figure 4. Typical titration curve obtained after voltammogram treatment and signal extraction (e.g. 10606 C3, 2015) with 14 Cu-standard additions (5 or 4 replicates), 4 µM of SA, 0.01 M borate buffer (pH ~ 8.2).

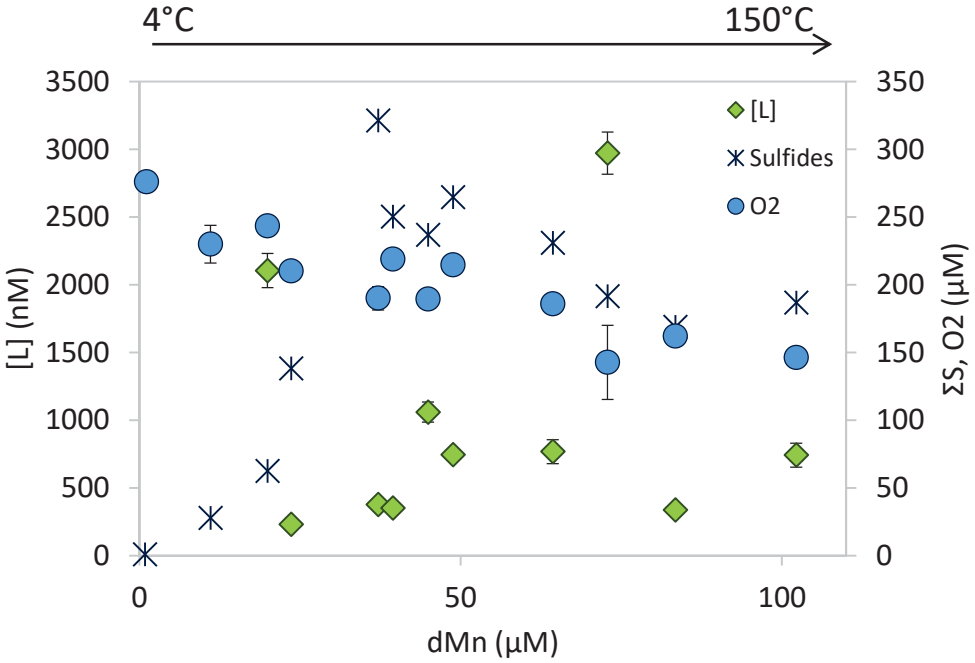

Figure 5. Concentrations of Cu-binding ligands and *in-situ* concentrations of free sulfides (ΣS = H_2S + HS^- + S^{2-}) measured with the CHEMINI analyzer at the main smoker of Aisics in 2015 (dive 02598). Blue dots refer to the *in-situ* concentrations of dissolved oxygen (O_2) measured by the Optode (Aanderaa). The linear relationship between temperature and dMn is T (°C) = 1.43(dMn) + 4; r^2 = 0.99 **(**Figure S4**)**, where the intercept refers to the deep seawater temperature. Errors bars for [L] are summarized in Table 1.

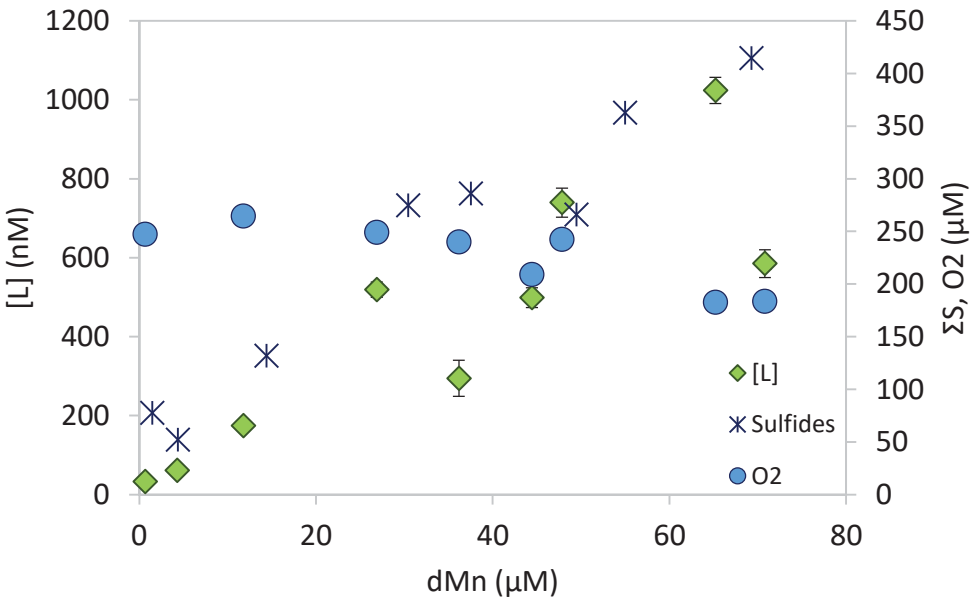

Figure 6. Concentrations of Cu-binding ligands ([L], dive 10606) and *in-situ* concentrations of free sulfides ($\Sigma S = H_2S + HS^- + S^{2-}$) measured with the CHEMINI analyzer at the main smoker of Y3 in 2014. The linear relationship between temperature and dMn is T (°C) = 1.35(dMn) + 4; $r^2 = 0.99$ (Figure S5).

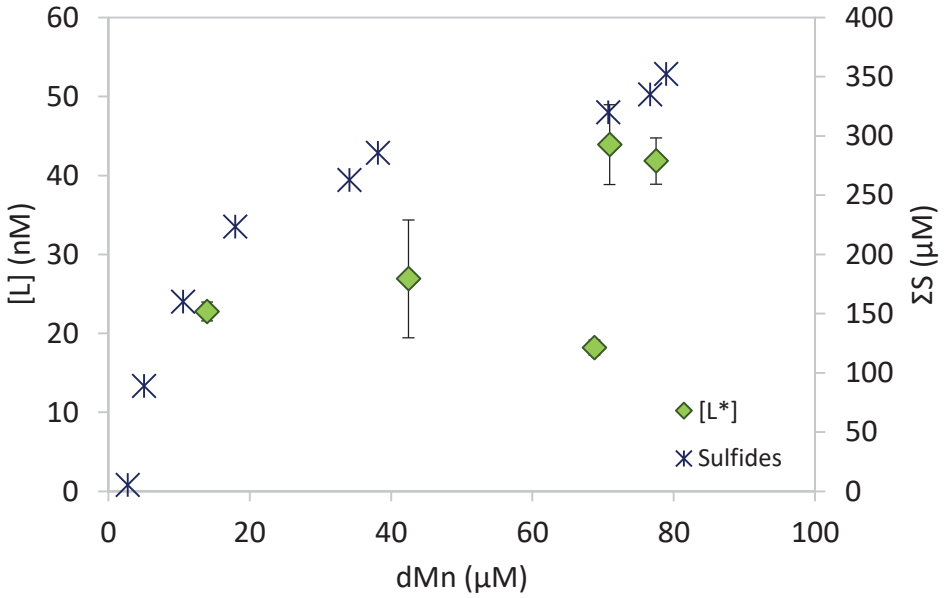

Figure 7. Concentrations of Cu-ligands and *in-situ* concentrations of free sulfides ($\Sigma S = H_2S + HS^- + S^2$) measured with the CHEMINI analyzer at the main smoker of Aisics in 2016. ΣS can be plotted as a function of dMn thanks to the linear relationship T (°C) = 1.47(dMn) + 4; $r^2 = 0.94$ (Figure S6).